1-1-2011

Pulmonary Particle Deposition in Relation to Age, Body Weight, and Species

Lisa M. Weber
University of Denver

Pulmonary Particle Deposition in Relation to Age, Body Weight, and Species

Abstract

As a result of dissimilarity in lung morphometry and physiological conditions, therapeutic aerosol particles deposit differently in humans of various ages and body weights. These particles also deposit differently in non-human species that are often utilized in inhalation and dosing studies. The focus of this work is to determine the optimal particle size and deposition (traditional efficiency and volume-weighted) of therapeutic particles in humans of both genders ranging in age from 3 months old to 21 years old and three non-human species (*B6C3F$_1$* mouse, Long-Evans hooded rat, and Beagle dog). This study finds that in humans, both optimal particle size and volume-weighted deposition are age and weight dependent; as age and weight increase, optimal particle size and deposition increase. Also, for all ages, breathing rates that are lower than normal enhance volume-weighted deposition and shift optimal particle size. Additionally, a rigorous sensitivity analysis of breathing rate and particles diameter on deposition shows that at normal breathing rates, sensitivity to breathing rate is greater than sensitivity to particle diameter for young children, but sensitivities to both become similar as age/body weight increase. At optimal breathing rates, the sensitivity to both breathing rate and particle diameter are lowest at the optimal breathing rates for children; for healthy adults, however, there is no apparent difference in sensitivity at normal and optimal breathing rates. This study also found that the mouse represents infants and young children relatively well, the rat represents older children relatively well, and the canine likely represents adolescents well. In addition, numerous studies postulate that the use of heliox instead of air will improve deposition as a result of the differences in density and dynamic viscosity; therefore, this study evaluates the effects of heliox based upon the differences in these properties. The results indicate that based on these properties, heliox does not appear to have any significant effect on deposition.

Document Type

Thesis

Degree Name

M.S.

Department

Mechanical Engineering

First Advisor

Corinne Lengsfeld, Ph.D.

Second Advisor

Peter Laz

Third Advisor

Bradley Davidson

Keywords

Animals, Deposition, Breathing rate, Lung, Particle, Alveolar, Particle size

Subject Categories

Biomedical Engineering and Bioengineering | Engineering

PULMONARY PARTICLE DEPOSITION IN RELATION TO AGE, BODY WEIGHT, AND SPECIES

A Thesis

Presented to

the Faculty of Engineering and Computer Science

University of Denver

In Partial Fulfillment

of the Requirements for the Degree

Master of Science

---

by

Lisa M. Weber

August 2011

Advisor: Dr. Corinne Lengsfeld

Author: Lisa M. Weber
Title: PULMONARY PARTICLE DEPOSITION IN RELATION TO AGE, BODY WEIGHT, AND SPECIES
Advisor: Dr. Corinne Lengsfeld
Degree Date: August 2011

ABSTRACT

As a result of dissimilarity in lung morphometry and physiological conditions, therapeutic aerosol particles deposit differently in humans of various ages and body weights. These particles also deposit differently in non-human species that are often utilized in inhalation and dosing studies. The focus of this work is to determine the optimal particle size and deposition (traditional efficiency and volume-weighted) of therapeutic particles in humans of both genders ranging in age from 3 months old to 21 years old and three non-human species (*B6C3F$_1$* mouse, Long-Evans hooded rat, and Beagle dog). This study finds that in humans, both optimal particle size and volume-weighted deposition are age and weight dependent; as age and weight increase, optimal particle size and deposition increase. Also, for all ages, breathing rates that are lower than normal enhance volume-weighted deposition and shift optimal particle size. Additionally, a rigorous sensitivity analysis of breathing rate and particles diameter on deposition shows that at normal breathing rates, sensitivity to breathing rate is greater than sensitivity to particle diameter for young children, but sensitivities to both become similar as age/body weight increase. At optimal breathing rates, the sensitivity to both breathing rate and particle diameter are lowest at the optimal breathing rates for children; for healthy adults, however, there is no apparent difference in sensitivity at normal and optimal breathing rates. This study also found that the mouse represents infants and young children relatively well, the rat represents older children

relatively well, and the canine likely represents adolescents well. In addition, numerous studies postulate that the use of heliox instead of air will improve deposition as a result of the differences in density and dynamic viscosity; therefore, this study evaluates the effects of heliox based upon the differences in these properties. The results indicate that based on these properties, heliox does not appear to have any significant effect on deposition.

ACKNOWLEDGEMENTS

I would like to thank my advisor, Dr. Corinne Lengsfeld, for all of her guidance and assistance during this process and constantly pushing me to do better. It has been a long and tedious journey.

I would also like to thank my lab group, friends, and family for their support and encouragement during times of extreme frustration and on those days when I felt like I didn't want to continue. I thank my dog, Dakota, for his endless loyalty and all of his cuddles exactly when I needed them.

Most of all, I would like to thank my mother for taking care of me when I broke my leg and encouraging me to keep working hard. She constantly reminded me, even when I felt less than capable and was constantly aggravated because I couldn't walk without crutches, that I am an intelligent, motivated, and fully capable person who can overcome adversity and achieve my goals. Thanks, Mom, for helping me to keep my focus.

TABLE OF CONTENTS

TABLE OF FIGURES

TABLE OF TABLES

TABLE OF VARIABLES

A	Age	yrs
A_c	Airway cross-sectional area	m^2
BF	Breathing frequency	min^{-1}
C_c	Cunningham slip correction factor	---
D	Airway diameter	m
D_d	Particle diffusion coefficient	$m^2 \cdot s^{-1}$
d	Particle diameter	m
d_{ae}	Aerodynamic diameter	m
$d_{optimal}$	Optimal particle diameter	m
FRC	Functional residual capacity	ml
F_{vi}	Adjusted cumulative volume fraction available	---
g	Acceleration due to gravity	$m \cdot s^{-2}$
k	Boltzmann constant	$J \cdot K^{-1}$
L	Airway length	m
MV	Minute volume (breathing rate)	$L \cdot min^{-1}$
N	Number of airways in lung generation	---
N_{Gen}	Number of particles that deposit in lung generation	---
N_{Tot}	Total number of particles	---
P	Total probability of deposition	---
p	Total probability exponent	---
P_i	Probability of inertial impaction	---
P_d	Probability of Brownian diffusion	---
P_s	Probability of gravitational sedimentation	---
R	Airway radius	m
Re_f	Fluid Reynolds number	---
Re_p	Particle Reynolds number	---
S	Sensitivity	---
SG	Specific gravity	---
Stk	Stokes number	---
T	Temperature	K
t	Time in lung generation	s
TLC	Total lung capacity	ml
TV	Tidal volume	ml
U_o	Fluid velocity	$m \cdot s^{-1}$
VWD	Volume-weighted deposition	---
$v_{settling}$	Particle settling velocity	$m \cdot s^{-1}$
W	Body weight	kg
x_d	Root mean square displacement	m
x_s	Settling distance in lung generation	m
Δ	Brownian motion probability factor	---
θ	Branching angle	º

κ	Gravitational sedimentation probability factor	---
λ	Mean free path	m
μ	Dynamic viscosity	$kg \cdot m^{-1} \cdot s^{-1}$
ν	Kinematic viscosity	$m^2 \cdot s^{-1}$
π	Mathematical constant	---
ρ_f	Fluid density	$kg \cdot m^{-3}$
ρ_p	Particle density	$kg \cdot m^{-3}$
σ	One standard deviation	---

CHAPTER ONE: INTRODUCTION

1.1 Motivation and Background

There are numerous non-invasive drug delivery routes available today, which include pulmonary, oral, buccal, nasal, vaginal/uterine, ocular, and transdermal (Kulkarni 2010). Each of these has some advantages and disadvantages compared to the others. Utilization of the respiratory tract for the treatment of respiratory diseases and as a route for systemic drug delivery has many advantages over the other non-invasive delivery methods for a few reasons. Rapid absorption via the respiratory tract is facilitated by the large surface area of the lung due to the substantial number of terminal bronchioles and alveoli, as well as the rich blood supply (which is accessible through extremely thin alveolar epithelium in close contact with the bloodstream) (Kulkarni 2010, Gupta and Hickey 1991). The surface area and rich blood supply contribute to a high rate of "therapeutic action" with reduced dosing when compared to delivery via other systemic routes or delivery of oral drugs with poor bioavailability (Kulkarni 2010). In addition, the respiratory tract does not have the extreme pH and metabolic enzymes found in the gastrointestinal tract, which can cause degradation and breakdown of medication (Kulkarni 2010, Wang, Siahaan and Soltero 2005). Furthermore, with pulmonary drug delivery there is not an issue with first-pass metabolism (primarily through the liver) that occurs with oral delivery and causes a reduction in bioavailability (Kulkarni 2010, Wang, Siahaan and Soltero 2005, Gupta and Hickey 1991). Also, systemic side effects may possibly be lower for pulmonary drug delivery than for oral

delivery because more tissue throughout the body is exposed to the medication with oral delivery (Gradoń and Marijnissen 2003). Because of these advantages, delivery of therapeutic particles for respiratory diseases by means of inhaled aerosols has become extremely common.

Although these benefits exist for drug delivery via the lung, the efficiency and efficacy of medication deposition utilizing this method are dependent upon and critically affected by numerous parameters. These parameters include spray properties, particle properties, physiological factors, and the morphometry of the respiratory system (Phalen 2009, Finlay 2001, Ruzer and Harley 2005, Xu and Yu 1986, Kim 2009). The respiratory system consists of "generations" of airways that begin with the trachea, which is considered to be generation 0. As the airways branch from the trachea to the deep lung, the generation number increases. The structure of the lung, including the lung generations and airway dimensions, are often referred to as lung morphometry. Figure 1 provides a visual representation of the branching structure and labeling scheme of the human lung. Understanding the branching structure of the lung is important when evaluating deposition of particles in particular lung regions.

A high deposition percentage of therapeutic particles in the appropriate generations of the lung is imperative when treating a particular disease, and as a result maximizing the particle deposition is essential when optimizing pulmonary drug delivery. Optimizing deposition is critical because it is estimated that 50% of school-aged currently receive little or no therapeutic effect from pressurized metered-dose inhaler (pMDI) devices (Pedersen, Dubus and Crompton 2010).

When comparing the parameters that deposition is dependent upon, it is apparent that the primary factors that are capable of being manipulated to optimize drug delivery are the particle properties. Aerodynamic diameter plays a critical role in particle deposition and is one of the most convenient particle properties to evaluate and adjust to determine optimal deposition.

Figure 1: Visual representation of branching structure of the human lung (Kleinstreuer, Zhang and Donohue 2008)

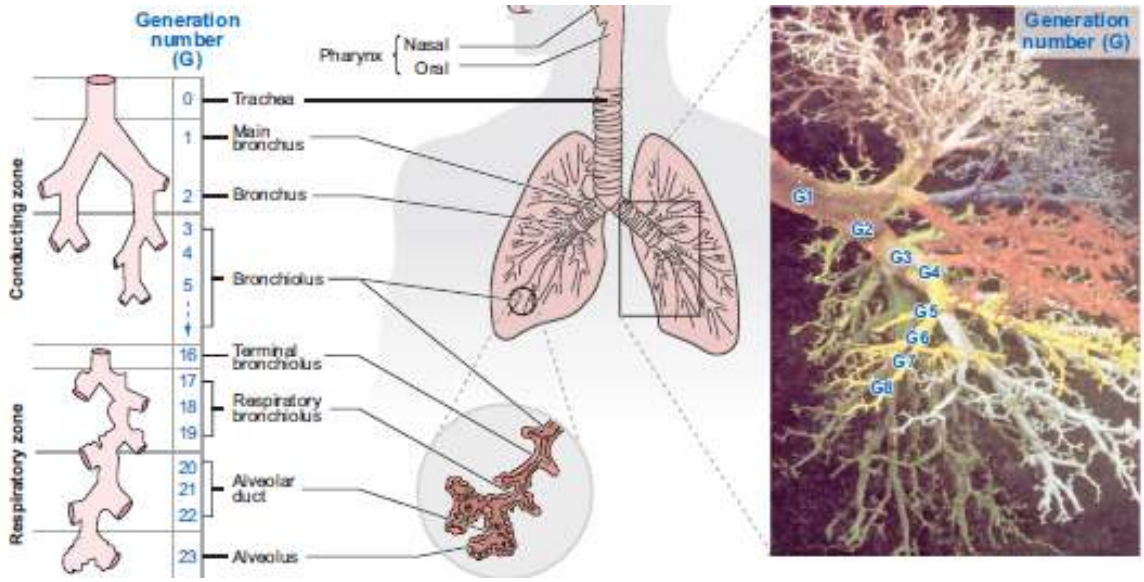

Physiological factors and respiratory system morphometry also affect particle deposition (Gradoń and Marijnissen 2003). Other than respiratory rate, these factors cannot be adjusted or manipulated to optimize deposition; additionally, these factors vary between individuals or are not consistent from infants to adults. As infants grow and their body mass increases, their respiratory system also continues to increase in size and develop. As a result, the morphometry of the lung is continually changing until growth stabilizes. Studies have

shown that the terminal bronchioles are already developed at birth, but that the respiratory airways (respiratory bronchioles, alveolar ducts, alveoli) continue to develop (Hofmann 1982, Dunhill 1962, Davies and Reid 1970). Not only does the respiratory system increase in size as body mass increases, but the number of alveoli and respiratory airways continue to increase as well. As a result studies have shown that infants and young children have a different number of lung generations than adults as a result of this (Finlay, Lange, et al. 2000, Ménache, et al. 2008, Dunhill 1962). Also, the lung growth in children is not linear and the largest growth rate occurs in the first two years after birth (Thurlbeck and Angus 1975). Since lung morphometry, an important factor in particle deposition, changes substantially from infancy to adulthood, there is also a high likelihood that particle deposition varies in infants, children, and adults (Finlay 2001, Xu and Yu 1986, Ruzer and Harley 2005). In addition, physiological factors such as breathing frequency, tidal volume, and respiratory rate also vary as a function of age (Finlay 2001, Phalen, Oldham and Beaucage, et al. 1985). All of these parameters contribute to particle deposition and as a result, it is necessary to determine the optimum particle diameter for deposition in infants and children as well as adults.

Furthermore, animal models are frequently used to model humans in an array of scientific studies, including inhalation studies (Phalen, Oldham and Wolff 2008). These animal models are often used in these health-related studies and the data is then extrapolated to humans because of the limited ability to test on humans (Martonen, Zhang and Yang 1992). However, physiological factors and lung structure in other species can vary substantially from humans. For example, respiratory bronchioles are not present in rats or

mice, which will possibly affect particle deposition (Phalen, Yeh and Schum, et al. 1978, Bal and Ghoshal 1988). Additionally, the number of lung generations present in different mammalian species that are used for lung studies is not always the same as in humans (Oldham and Robinson 2007, Maina and Gils 2001, Weinberg, et al. 2005). For example, the 21-yr old human lung model evaluated in this study has 24 lung generations and the Beagle dog lung model has 29 lung generations. Moreover, many of the species that are used in lung studies have substantial differences in lung shape from humans. For instance, some studies have shown that many mammalian species (including rats, rabbits, and dogs) have lungs structures that are more monopodial whereas human lungs are typically described as being nearly dichotomous (Phalen, Oldham and Wolff 2008, Phalen, Yeh and Schum, et al. 1978, Weinberg, et al. 2005, Phalen and Oldham 1983). Figure 2 illustrates this difference. This is because these species have elongated chest cavities while the chest cavity of the human is relatively spherical (Phalen, Oldham and Wolff 2008).

Another difference is that the branching in humans is typically much more symmetrical than that of many laboratory animals (Dahl, et al. 1991), which is also clearly shown in Figure 2; the human lung has two lobes that are very similar in size and shape, but the Beagle dog has one primary lobe and the other lobe is nearly non-existent. Since these animal models are frequently used to model humans, it is important to also determine particle deposition in the various species that are used in inhalation and dosing studies to see how accurately they represent the deposition in the human. Since there are differences in lung morphometry from infancy to adulthood and as a result depositions are not the same, it

is also useful to determine if different animal models more accurately represent humans at different growth stages.

Figure 2: *In situ* casts of the tracheobronchial tree of: (a) a healthy 60-year-old man and (b) a healthy 10-kg laboratory beagle to illustrate the monopodial structure (Phalen, Oldham and Wolff 2008)

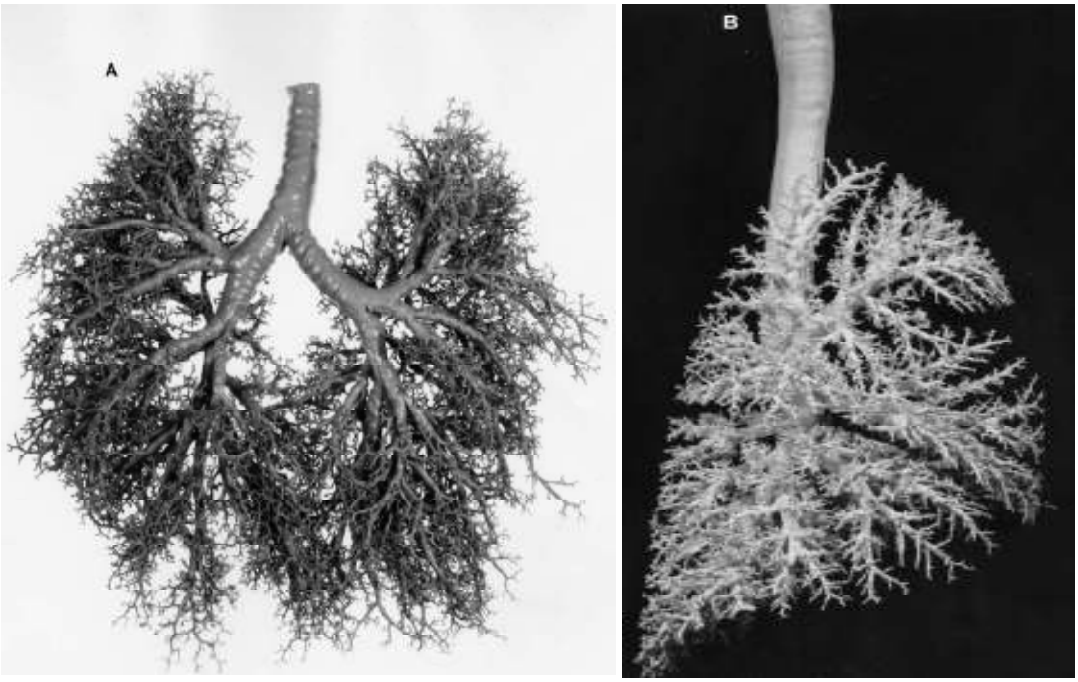

Numerous studies compared differences in human lung morphometry as a function of age (Hofmann 1982, Ménache, et al. 2008, Thurlbeck and Angus 1975) as well as particle deposition as a function of age (Phalen and Oldham 2001, Finlay, Lange, et al. 2000, Xu and Yu 1986, Phalen, Oldham and Beaucage, et al. 1985, Asgharian, Ménache and Miller 2004, Yu, et al. 1992, Oldham and Robinson 2006). There have also been several studies that compare the lung morphology of human adults and various mammalian species (Bal and Ghoshal 1988, Phalen, Yeh and Raabe, et al. 1973, Phalen, Yeh and Schum, et al. 1978,

Schlesinger and McFadden 1981, Phalen and Oldham 1983, Phillips and Kaye 1995). When it comes to deposition, many studies have determined deposition solely in one species or compared deposition between various animal species (Hsieh, Yu and Oberdörster 1999, Schmid, et al. 2008, Weinberg, et al. 2005, Kliment, Libich and Kaudersova 1972, Kliment 1974, Oldham and Robinson 2007, Schum and Yeh 1980). There have, however, only been a few studies that compare deposition in various species to deposition in humans (Dahl, et al. 1991, Martonen, Zhang and Yang 1992, Schlesinger 1985, Martonen, Katz and Musante 2001).

There are, however, no known studies that include both humans of various ages and multiple species. Additionally, all the studies to date report optimal particle sizes based on deposition efficiency based on number of particles with no regard to the therapeutic volume of drug delivery. The purpose of this study is to inclusively investigate humans and multiple species, utilizing the same deposition model, to allow for a more direct comparison. This study will also highlight the differences in optimal particle size based on deposition efficiency compared to a volume-averaged deposition. The goal of the work is to provide guidance on the optimal particle size for various ages and species. Additionally, this work evaluates the effect of breathing rate on deposition and optimal particle size.

This work hypothesizes that the optimal particle size and breathing rate for deposition will be significantly smaller for the infant than for the adult. More specifically, that optimal particle size and breathing rate will be dependent upon body weight. It is also hypothesized that the delivered dose (volume-weighted deposition) and optimal particle size will differ significantly between various animal species and humans, thereby calling into question the

use of these animal models to determine medication dosing in humans. Also, it is hypothesized that heliox will lead to enhanced deposition when compared to air as a result of differences in density and dynamic viscosity.

This study uses lung morphometry, respiratory conditions, lung volumes, fluid dynamics, and a static statistical probabilistic model to determine deposition of particles in the pulmonary region of the lung via sedimentation, impaction, and Brownian motion. Details regarding all of the models and calculations performed in this study will be discussed in the Chapter 2 and deposition results are described in Chapters 3-5. These models are used for a few reasons. Models can provide valuable information regarding a range of parameters before performing possibly difficult and expensive experimentation. Also, rarely are parents willing to subject their infants and young children to radiolabelled deposition studies.

CHAPTER TWO: METHODS

2.1 Human Respiratory Conditions and Morphometry Models

Airway lengths and diameters as a function of lung generation are needed to perform particle deposition calculations. There are many adult lung morphometry models with complete airway dimensions available to utilize in particle deposition calculations; however, complete lung models for infants and children are considerably more scarce. Many of the available deterministic models were considered in this study when choosing appropriate lung morphometry models to use for infants, children, and adults.

The symmetrical dichotomous lung morphometry model (Model "A") provided by Weibel (1963) is one of the most well known and frequently used models available for the adult. Although this model is commonly used, it is known for under predicting the diameters of the conducting airways as well as the diameters and lengths of the alveolar airways (Finlay 2001). An additional work revised the small airway dimensions in the alveolar region and modified the generation where the respiratory bronchioles begin (Haefeli-Bleuer and Weibel 1988), but the issue with the undersized conducting airway diameters has not been addressed. The lung dimensions in this model are at a volume of 4800 ml (or ¾ TLC), and thus the model considers the volume of the lung at maximum inflation, or total lung capacity (*TLC*), of the adult to be 6400 ml (Weibel 1963). Often times lung dimensions are scaled to functional residual capacity (*FRC*), which is the volume still present in the lung after each breath has been exhaled. The Weibel model is commonly scaled because FRC in

an adult male is approximately 3100 ml (Finlay 2001) and a lung volume of ¾ *TLC* is not especially useful in calculations. In addition to the Weibel model, several other complete morphometric lung models are also available for the adult (Yeh 1980, Yeh and Schum 1980, Horsfield and Cumming 1968).

As previously mentioned, there are significantly fewer models with complete lung morphometry for infants and children. Several of the studies that do include infants or children have only scaled the airway geometries provided by one or more adult models (such as Weibel "A") instead of determining infant and children morphometry based on casting and extrapolation (Finlay, Lange, et al. 2000, Hofmann, Martonen and Graham 1989). In addition, many of the studies that provide airway data based upon casting often include only morphometry for conducting airways and the airways distal to the terminal bronchiole have not been incorporated (Ménache, et al. 2008).

It is difficult to reasonably compare many of the adult models available, including the Weibel Model "A" morphometry, to the models of children because they are nearly all constructed using different methods. Since a variety of different ages will be taken into consideration in this study, lung models provided by Ménache, et al. (2008) will be utilized in all calculations. The lung geometries in these models are provided in Appendix A. The models provided by Ménache, et al. (2008) are all constructed using the same method for consistency and include both males and females of various ages, which are summarized in Table 1. The Ménache, et al. (2008) lung morphometry models assume that the human lungs are symmetrical, so the number of airways doubles each time branching occurs.

Table 1: Information regarding human lung casts (Ménache, et al. 2008)

Age (yr)	Gender	Weight (kg)	Height (cm)	BMI
0.25	F	5.9	66.0	13.5
1.75	M	9.0	71.1	17.8
1.92	M	9.1	94.0	10.3
2.33	F	12.2	94.5	13.7
3.00	F	13.6	109.0	11.4
8.67	M	26.0	118.0	18.7
9.42	M	40.9	143.0	20.0
14.00	F	51.0	175.2	16.6
14.08	F	56.0	147.0	25.9
18.00	M	52.0	135.0	28.5
21.00	M	67.0	177.8	21.2

Using the Ménache, et al. (2008) lung models will allow for a wide range of ages to be evaluated and will contribute to a more reasonable comparison between deposition results. However, all of the airway dimensions in these models assume that the lung is at *TLC*. This is not an acceptable assumption when analyzing particle deposition because the lung is never actually at *TLC*. Therefore, these models must be scaled so that the airway dimensions more accurately represent the volume of the lung when breathing. In this study, the lung models have been scaled to $FRC + TV/2$, where *TV* is the tidal volume (average volume inhaled or exhaled when breathing). This scaled volume is the average volume in the lung halfway through one breath. Only diameters are assumed to constrict as a function of the decrease in volume that occurs when scaling the lungs down from *TLC*. Consequently, the diameters have been scaled down proportionally; the airway lengths are assumed to remain constant. It is important to mention that in this study, the airways in each generation are considered to be cylinders and the presence of alveoli and their effect on fluid flow is neglected.

Since particle deposition is not only dependent upon morphometry, but is also dependent upon physiological factors such as respiratory conditions and lung volumes, these

must also be determined. The physiological parameters that are required include breathing frequency (*BF*), *TV*, *FRC*, and *TLC*. *BF* and *TV* are dependent upon age and are used to determine minute volume (*MV*), or breathing rate. They are calculated using the following analytical expressions presented in Hofmann (1982), where *A* is age in years.

$$TV\ (ml) = 21.7 + 35.13A - 0.64A^2 \qquad (1)$$

$$BF(\mathrm{min}^{-1}) = \frac{15.17}{0.25A+0.5} + 11.75 \qquad (2)$$

These expressions were determined from numerous authors for tidal volumes and breathing frequencies obtained during rest. *FRC* and *TLC* are determined by utilizing numerous analytical expressions that are a function of age, body mass, height, or a combination of the three and averaging the results. Averaging a multitude of correlations provided by numerous sources should assist in removing variation caused by small sample numbers and/or bias by health state and provide consistent values that lie within a clinically acceptable range. The analytical expressions that are averaged are provided by Taussig, et al. (1997), Quanjer, et al. (1993), Stocks and Quanjer (1995), Cook and Hamman (1961), Gaultier, et al. (1979), Zeltner, et al. 1987, and Quanjer, et al. (1989). The values for *BF*, *TV*, *MV*, *FRC*, and *TLC* that are used in calculations are summarized in Table 2.

Table 2: Summary of human respiratory conditions and lung volumes

Age (yr)	Gender	BF (min^{-1})	TV (ml)	MV (L/min)	FRC (ml)	TLC (ml)
0.25	F	39	30	2.36	178	328
1.75	M	28	81	4.54	232	465
1.92	M	27	87	4.73	329	589
2.33	F	26	100	5.16	371	699
3.00	F	24	121	5.80	458	822
8.67	M	17	278	9.70	908	1990
9.42	M	17	296	10.09	1573	3243
14.00	F	16	388	12.06	2578	5362
14.08	F	16	389	12.09	1650	3533
18.00	M	15	447	13.20	1348	2871
21.00	M	14	477	13.73	3281	6656

Additionally, a variety of breathing frequencies are taken into consideration for males of three different ages (1.92-yr old, 9.42-yr old, and 21-yr old) to determine if both traditional and volume-weighted deposition efficiencies are affected by a change in breathing rate. Since the tidal volumes are different for each of these ages, the same breathing frequency value will not translate into the same breathing rate for each age, which is important to note since this will play a role in the results. The breathing frequencies that are evaluated are 0.5, 1, and 5 to 65 min^{-1} at 5 min^{-1} intervals. When the general range of where the maximum deposition efficiency is located, the results are then refined to determine a more accurate maximum efficiency and the corresponding breathing rate. For the 1.92-yr old, these breathing frequencies translate into breathing rates from 0.087 L/min to 11.28 L/min. For the 9.42-yr old, the breathing frequencies translate into breathing rates from 0.30 L/min to 38.46 L/min. For the 21-yr old, the breathing frequencies translate into breathing rates ranging from 0.48 L/min to 62.03 L/min.

For these three models, a sensitivity analysis is also performed to determine the sensitivity of volume-weighted deposition to both breathing rate and particle diameter.

Sensitivity is determined by evaluating the change in the performance parameter, normalized, to the change in the input variable, normalized. The sensitivity is determined by

$$S = \frac{\frac{Y_i - Y_{i-1}}{Y_i}}{\frac{X_i - X_{i-1}}{X_i}} \qquad (3)$$

where Y is the performance parameter and X is the input variable. For example, when performing the sensitivity of volume-weighted deposition to breathing rate, the performance parameter Y is the volume-weighted deposition and the input variable X is the breathing rate. The larger the sensitivity value, the more sensitive the performance parameter is to the input variable.

2.2 Animal Respiratory Conditions and Morphometry Models

Various animal species are frequently used in inhalation and respiratory studies; thus, it is relevant to determine in each case whether or not these species adequately represent humans. Particle deposition calculations will be performed for a subset of animal models and compared with the human results. To perform these calculations, lung morphometry and respiratory conditions are also required for each species that will be compared to humans in this study.

Obtaining lung morphometry as a function of lung generation for various non-human species is difficult because the quantitative data available are limited. Since respiratory conditions in many species are dependent upon body weight, it is necessary to find respiratory conditions and lung morphometry for an animal of same weight and same or similar species. Therefore, even if lung morphometry is available, finding appropriate

respiratory conditions for each species can also be challenging because this information is equally as scarce. As a result of this, the animal models that are utilized in this study include the *B6C3F1* mouse, the Long-Evans hooded rat, and the Beagle dog because both lung morphometry and respiratory conditions are available. The cast information for the animal species in this study is summarized in Table 3.

Table 3: Information regarding animal lung casts

Model	Age (mo)	Gender	Weight (g)
$B6C3F_1$ Mouse[a]	Not Stated	Not Stated	25.6
Long- Evans Rat[b]	12	F	330.0
Beagle Dog[c]	17	M	11,600.0

[a] from Phalen (1991). [b] from Yeh (1979). [c] from Yeh (1980).

For the *B6C3F1* mouse, lung morphometry is provided by Phalen (1991). The respiratory conditions, *FRC*, and *TLC* for the mouse are determined using correlations provided by Hsieh, Yu and Oberdörster (1999). For the Long- Evans rat, lung morphometry and *TLC* are provided by Yeh (1979). Respiratory conditions and *FRC* for the rat are determined using correlations provided in Hsieh and Yu (1999). Even though these correlations are for Fischer rats, body weight between the two rat strains are similar and therefore it is assumed that respiratory conditions and *FRC* for the Fischer rats are applicable to Long-Evans rats. This assumption is made because lung morphometry for the Fischer rat and respiratory conditions for an appropriately-sized Long-Evans rat are not available. For the Beagle dog, lung morphometry is provided by Yeh (1980). Respiratory conditions and lung volumes are estimated using data provided by Mauderly (1974). The lung geometries

for these three animal species are provided in Appendix A. The respiratory conditions, and lung volumes for the three animal species used in this study are summarized in Table 4.

Table 4: Summary of animal respiratory conditions and lung volumes.

Model	BF (min^{-1})	TV (ml)	MV (L/min)	FRC (ml)	TLC (ml)
$B6C3F_1$ Mouse	160[a]	0.189[a]	0.0605[a]	0.629[a]	0.976[a]
Long- Evans Rat	120[b]	2.23[b]	0.535[b]	8.09[b]	14.1[c]
Beagle Dog	19[d]	244[d]	9.27[d]	545[d]	1363[d]

[a] from Hsieh, Yu and Oberdörster (1999). [b] from Hsieh and Yu (1999). [c] from Yeh (1979).
[d] from Mauderly (1974).

All of the animal lung morphometry models are also based upon a lung at *TLC*. Therefore, the animal models are also scaled from *TLC* to a lung volume of $FRC + TV/2$. Once again, the diameters are scaled appropriately and the lengths are assumed to remain constant.

2.3 Fluid Dynamics and Particle Deposition Model

In this study, all calculations will be performed with air and heliox (80/20). Heliox is a gas mixture containing helium and oxygen that has a viscosity that is higher than air and a density that is lower than air. The ratio can vary, but this study considers heliox that is 80% helium and 20% oxygen by volume. The gas mixture is frequently used in critically ill patients because multiple studies suggest that it lowers resistance and increases particle deposition in the deep lung (Corcoran and Gamard 2004); therefore, the effects of air and heliox on particle deposition are evaluated and compared in this study.

This study will evaluate deposition of particles with a geometric particle diameter *d* from 1.0 μm to 10.0 μm in 1 μm increments. A number of assumptions relating to the lungs,

the fluid (air or heliox), and the particles are made before beginning particle deposition calculations. First, it is assumed that no dilation or contraction of the lung occurs. Also, all deposition is assumed to occur on inhalation. The airways are assumed to be cylindrical and are only scaled radially, not longitudinally. It is assumed that the particles are spherical and monodisperse, meaning all of the particles are the same size so that no particle distributions need to be taken into consideration. In addition, it is assumed that the particles are homogeneously distributed throughout the inhaled volume. All of the particles are not forced to deposit or see each airway generation. Instead, this study models the inhalation more realistically, where a particular volume is inhaled and the initial section of the volume passes through more generations than the final segment of that volume. It is assumed that the aerosol cloud is charge neutral and electrostatic effects are negligible. This is a reasonable assumption because the high humidity in the lung neutralizes the charge of the particles (Finlay 2001). This study also assumes that the particle growth by hygroscopic effect is negligible. It is assumed the flow is incompressible, which is considered a reasonable approximation in most cases of aerosol inhalation because the velocities are typically below 100 m/s and temperature differences are typically below 30K (Finlay 2001).

Also, the spray velocity is assumed to be the same as breathing rate. In addition, there is considered to be no spray angle, so the fluid and particle velocities are assumed to be parallel to the airway walls. Finally, buccal and nasal depositions are not taken into consideration as this study only evaluates deposition that occurs from the trachea to the deep lung.

Various fluid and particle properties are required for deposition calculations. The air temperature is assumed to be 37ºC (310.15K), which is the temperature of the human body. The particle density ρ_p used in this study is 1.0×10^3 kg/m^3. For air, the following properties are assumed: the density ρ_f is 1.2 kg/m^3, the dynamic viscosity μ is 1.90×10^{-5} kg/m-s, and the mean free path λ is 0.072 μm at 37ºC and 1 atm (Finlay 2001). For heliox, the density and dynamic viscosity are provided by Praxair and are 0.4 kg/m^3 and 1.98×10^{-5} kg/m-s, respectively. The mean free path for heliox is assumed to be the same as air. In addition, the branching angle (of the airways in each generation is assumed to be 38.24º (Finlay 2001).

Particle deposition, particle motion, and fluid dynamics calculations utilized in this study are described by Finlay, 2001. Particle deposition is determined using a statistical mathematical model. Particle motion and fluids dynamics calculations are required to evaluate particle deposition. For particle motion, it is assumed that there is a single particle with a density much larger than the fluid density (Finlay 2001); this particle is assumed to be isolated, so all interactions between particles are neglected. This is generally true except for some dry powder inhalers.

First, it is essential to know the fluid velocity in a particular lung generation. The fluid velocity U_0 (in m/s) is

$$U_0 = \frac{MV}{A_c \cdot N} \qquad (4)$$

where MV is minute volume (or breathing rate) in m^3/s, A_c is the cross-sectional area of an airway in that generation in m^2, and N is the number of airways in that generation. Once the fluid velocity is known, the Reynolds numbers for the particle and the fluid can be

determined. The Reynolds numbers display the importance of inertial forces to viscous forces and are nondimensional. The particle Reynolds number Re_p is necessary to ascertain the validity of numerous equations and is

$$Re_p = \frac{U_0 d}{\nu} \qquad (5)$$

where d is particle diameter in m and ν is the kinematic viscosity of air in m^2/s, which is defined as

$$\nu = \frac{\mu}{\rho_f} \qquad (6)$$

where μ is the fluid dynamic viscosity in kg/m·s and ρ_f is the fluid density in kg/m^3. The fluid Reynolds number Re_f is necessary to evaluate the fluid flow regime for a particular generation and is

$$Re_f = \frac{U_0 D}{\nu} \qquad (7)$$

where D is the diameter of the airway in that generation in m. The fluid flow regime is laminar when $Re_f < 2300$. Under normal breathing conditions, the flow is laminar in all generations of the lung.

Aerodynamic diameter is often used instead of geometric diameter to describe a particle in an aerosol. Aerodynamic diameter d_{ae} is given as

$$d_{ae} = d\sqrt{SG} \qquad (8)$$

where d is the particle diameter in m and SG is the specific gravity the particle, which is nondimensional. This equation is only valid when the Re_p is much less than 1 and d is much less than λ. Both of these conditions are satisfied in this study. Since the particle density that is chosen is about the same as the density of water, the aerodynamic diameters are

determined and are very nearly the same as the geometric diameters, thus there is no affect on the results.

Particle deposition occurs in the respiratory tract by three primary mechanisms: sedimentation, inertial impaction, and diffusion. Sedimentation is when the particles deposit in an airway because of gravitational settling. To determine the probability of sedimentation, the cross sectional area of the flow tube is observed with time. It is assumed that the entire area will move downward as a result of gravitational forces on particles homogeneously distributed within the area. The time for this motion will be determined by the velocity of the flow and the length of the generation. The area that falls below the wall of the tube will become the percentage of the particles deposited. Thus for sedimentation calculations, the fluid velocity profile is assumed to be laminar plug flow. In plug flow, the fluid velocity is the same across any cross-sectional area of the tube. When determining the probability of sedimentation, the terminal settling velocity (velocity at which the particle settles due to gravity) for each particle must be determined. The settling velocity $v_{settling}$ (in m/s) is

$$v_{settling} = \frac{C_c \rho_p g d^2}{18\mu} \quad (9)$$

where g is acceleration due to gravity in m/s^2, d is particle diameter in m, and C_c is the Cunningham slip correction factor and is nondimensional. This equation is also only valid when the Re_p is much less than 1 and d is much less than λ. The Cunningham slip correction factor is necessary when the particle diameter gets smaller and the mean free path is not much smaller than particle radii (Finlay 2001). The Cunningham slip correction factor is defined as

$$C_c = 1 + 2.25\frac{\lambda}{d} \qquad (10)$$

The distance in which the particle will settle in a particular generation x_s (in m) is given by

$$x_s = \nu_{settling} t \qquad (11)$$

where t is the residence time of a particle in that generation in s. It is also necessary to compute κ to determine sedimentation probability. The value of κ is

$$\kappa = \frac{3\nu_{settling} L}{4U_0 D}\cos\theta \qquad (12)$$

where L is the length of an airway in a particular generation in m and θ is the airway branching angle. The probability of gravitational sedimentation for laminar plug flow is

$$P_s = 1 - \frac{2}{\pi}\left[cos^{-1}\left(\frac{4}{3}\kappa\right) - \frac{4}{3}\kappa\sqrt{1 - \left(\frac{4}{3}\kappa\right)^2}\right] \qquad (13)$$

When using this equation, it is important to note that κ is only a real number when it is less than ¾. Due to this, P_s is frequently set to 1 when $\kappa \geq ¾$ because this indicates that it takes a particle longer to travel through the length of the tube than it does for it to travel the diameter of the tube perpendicular to the flow and therefore sedimentation will occur (Finlay 2001).

Particle deposition also occurs by means of inertial impaction. Deposition occurs via inertial impaction when there is curvature in an airway and the inertia of the particle is too great, resulting in a particle trajectory that no longer follows the fluid flow streamline causing the particle to deposit on the airway wall. Deposition as a result of inertial impaction primarily occurs as a result of airway bifurcations and inertial deposition probabilities have been well described by empirical relations developed over the past century. The Stokes number determines whether or not inertial impaction will occur and

therefore is necessary when evaluating the probability of deposition via impaction. The Stokes number *Stk* is nondimensional and is

$$Stk = \frac{U_0 \rho_p d^2 C_c}{18 \mu D} \qquad (14)$$

The probability of inertial impaction is given by Chan and Lippmann (1980) and is

$$P_i = 1.606 Stk + 0.0023 \qquad (15)$$

This expression was determined based on experimental data in lung casts that take into consideration the effects of the larynx and multiple generations (Finlay 2001).

Other than sedimentation and impaction, particle deposition also takes place as a result of Brownian diffusion. Very small particles have Brownian motion occur due to interactions with the molecules of the gas they are carried by. Brownian motion is when a particle collides with the molecules and random walk occurs. This is considered to be diffusion when this takes place with many particles. The root mean square displacement x_d (in m) describes the distance the particle travels due to Brownian motion and is

$$x_d = \sqrt[2]{2 D_d t} \qquad (16)$$

where D_d is the particle diffusion coefficient in m^2/s. The particle diffusion coefficient D_d is

$$D_d = \frac{kTC_c}{3\pi \mu d} \qquad (17)$$

where k is Boltzmann's constant (1.38×10^{-23} $J \cdot K^{-1}$) and T is the temperature in K (37 ºC=310.15K). To determine the probability of Brownian diffusion, Δ is

$$\Delta = \frac{kTC_c L}{3\pi \mu d U_0 R^2} \qquad (18)$$

where k is Boltzmann's constant and R is the radius of the airway in a generation in m. The probability of deposition due to Brownian diffusion assuming Poiseuille flow in a cylindrical tube is given by Ingham (1975) and is

$$P_d = 1 - 0.819e^{-14.63\Delta} - 0.0967e^{-89.22\Delta} - 0.0325e^{-228\Delta} - 0.0509e^{-125.9\Delta^{2/3}} \quad (19)$$

Inertial impaction is the dominant deposition mechanism in the larger airways and deposition via sedimentation is dominant in the alveolar region. Also, deposition via both impaction and sedimentation increases as the particle size is increased.

So far, the equations provided determine the probability of each of these deposition mechanisms occurring alone, which is unrealistic; in reality, these deposition mechanisms occur simultaneously in the lung. Consequently, an empirical relation that calculates the total probability of deposition by taking into consideration all three types of deposition is used. The total probability P is determined using

$$P = (P_i^{\,p} + P_s^{\,p} + P_d^{\,p})^{1/p} \quad (20)$$

where P_i is probability of impaction, P_s is the probability of sedimentation, P_d is the probability of Brownian motion, and the value of p (in the exponents) is assumed to be 2 in this study.

The ratio of x_d/x_s is useful for assessing how important diffusion is when compared with sedimentation. If $x_d/x_s < 0.1$, then diffusion becomes negligible and no longer needs to be taken into consideration. When diffusion is not taken into consideration, the total probability becomes

$$P = P_i + P_s - P_i P_s \quad (21)$$

Once the total probability of deposition is determined in each lung generation for each particle size, it is necessary to quantify the results in a way that is more applicable to dosing. Most studies assume that the particles move through the lung at the same time at an infinite particle density. This is both physically unrealistic and violates several of the assumptions used to develop the statistical models. It was instead chosen in this study to have each model inhale a normal tidal volume where the particles are homogenously distributed throughout the entire volume. The consequence of this is the need to tag particles to a particular segment of the tidal volume as the last segment of the tidal volume inhaled never reaches the deep lung. This is achieved using the following equation

$$F_{V_i} = 1 - \frac{\sum V_{i-1}}{V_{Total}} \qquad (22)$$

where i is the generation number, F_{Vi} is the fraction of the adjusted cumulative volume still available, V_{Total} is the total adjusted cumulative volume, and $\sum V_{i-1}$ is the sum of the adjusted volumes above that generation.

CHAPTER THREE: HUMAN CORRELATIONS AND DEPOSITION RESULTS

3.1 Introduction

Deposition calculations are performed for both males and females and consider a range of ages from 3-months old to 21-years old. A broad range of ages is considered to determine if the optimal particle size for alveolar deposition shifts as age increases. In addition, the relationship between deposition and factors other than age are evaluated. These factors include gender, weight, and height. Weight and height are both evaluated individually as well as combined in body mass index (BMI) since it accounts for both of these parameters.

Some studies suggest deposition is highly dependent upon breathing rate (Bennett 1996), so differences in breathing rate and the resulting affects on particle deposition for three different ages (1.92-yr old, 9.42-yr old, and 21-yr old) are also taken into consideration by varying breathing frequency. Since for a particular breathing frequency the corresponding breathing rate for each age will not be the same as a result of the differences in tidal volume, these breathing rate variations are also discussed. A sensitivity analysis is performed as well to determine the sensitivity of volume-weighted deposition to both breathing rate and particle diameter.

3.2 Methods

In the calculations with exclusively humans, volume-weighted deposition is determined for the alveolar region (AL) of the lung. The optimal particle size is the particle diameter at which the maximum volume-weighted deposition occurs. First, the volume-weighted deposition is determined from 1 μm to 10 μm in 1 μm increments. From this analysis, the specific region in which the maximum volume-weighted deposition occurs is discernable. Volume-weighted deposition is then determined in this specific region in 0.1 μm increments to determine the optimal particle size to the tenth of a micron.

This study ignores particles deposited in the conducting airways, generations 0-14, because cilia will move the therapeutic up and out of the lung and into the stomach; thus, little to no therapeutic effect will be obtained from these particles. Generations 15-18 are the respiratory bronchioles; the particle deposition in these generations is also ignored because rapid drug absorption and ideal target region for therapeutic effect is the alveolar region, consisting of generations 19-23 in the infant through 3-yr old and generations 19-24 in the 8-year old through 21-yr old. However, in the 21-yr old, the aerosol that is inhaled will never reach generation 24 because the cumulative adjusted volume of generation 23 in the adult is 675.2 cm^3 and the tidal volume is 477.2 cm^3. As a result of this, the aerosol that is inhaled will never surpass generation 23 and therefore generation 24 has been neglected in deposition calculations for the 21-year old. This only happens for the 21-yr old.

3.3 Results and Discussion

3.31 Volume-Weighted Deposition and Optimal Particle Size Relationships

Age, weight, height, and body mass index (BMI) are evaluated in this study to determine whether correlations exist between these parameters and volume-weighted deposition or optimal particle size. These results are displayed in Figures 3-9.

Figures 3 (a) and (b) show the relationships between age and weight to volume-weighted particle deposition, respectively. Figures 4 (a) and (b) show the relationships between height and BMI to volume-weighted deposition, respectively. Boundary limits (2σ) that are 2 standard deviations above and below the trend line are also shown on each graph. Based on the results, age and weight have significantly stronger relationships to volume-weighted deposition than BMI and height. This is evident by the larger scatter in the BMI and height data, lower r^2 values, and considerably broader 2σ limits of the BMI and height results. Because of this, height and BMI will not be used to describe volume-weighted deposition behavior. The results for BMI are not surprising because BMI typically is not used for children because it does not accurately represent them. CDC growth charts are used for children instead because they show what percentile a child is in relation to other children of the same age.

As seen in Figure 3 (a), the increase in volume-weighted deposition as a function of age between males and females appears to overlap until approximately 10 years of age. After 10 years of age, divergence in volume-weighted deposition between the two genders appears. This is not surprising because as age increases, growth rates between the two genders begin to differ from puberty through adulthood. It is also important to note that

based on these results, the rate of increase of volume-weighted deposition (Figure 3 (a) slopes) as a function of age tends to be higher for females than for males. This implies that for adult subjects, volume-weighted deposition in subjects of the same age will likely be slightly higher in a female than a male. However, the volume-weighted deposition for the 14.08-year old is outside of the 2σ bounds on three of these four figures. This implies that there is a possibility that it is an outlier and does not accurately represent the population, possibly skewing the result slightly. Without the 14.08-yr old included in the age versus volume-weighted deposition figure (Figure 3 (a)), the differences between volume-weighted deposition for males and females in relation to age becomes considerably less significant.

Figure 3 (b) demonstrates that significant overlap occurs between the males and females in relation to volume-weighted deposition as a function of weight. Because of this, it is possible to develop a relationship between volume-weighted deposition and body weight for humans in general and gender can be disregarded. Figure 5 demonstrates this relationship; notice the majority of subjects in this study fall within 2σ of this relationship despite their gender.

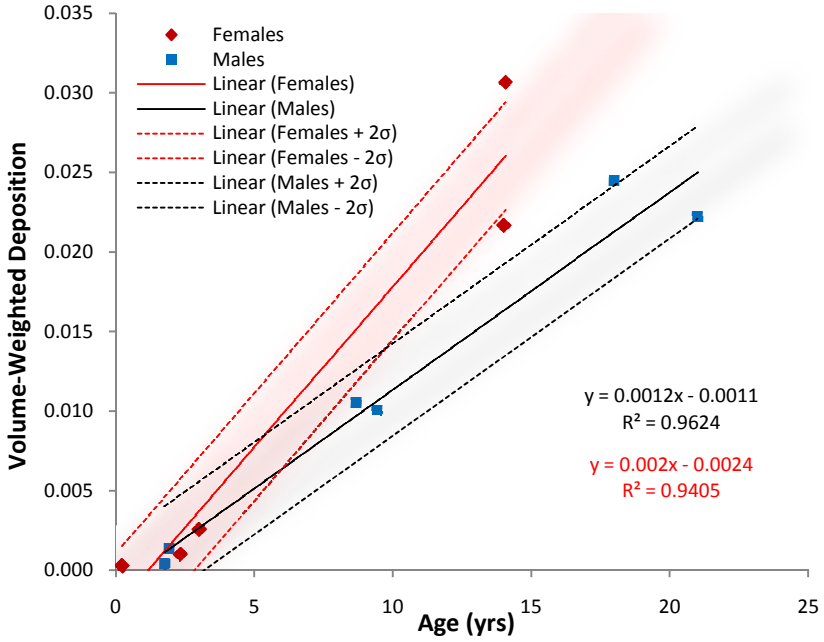

Figure 3: (a) Volume-weighted AL deposition as a function of age

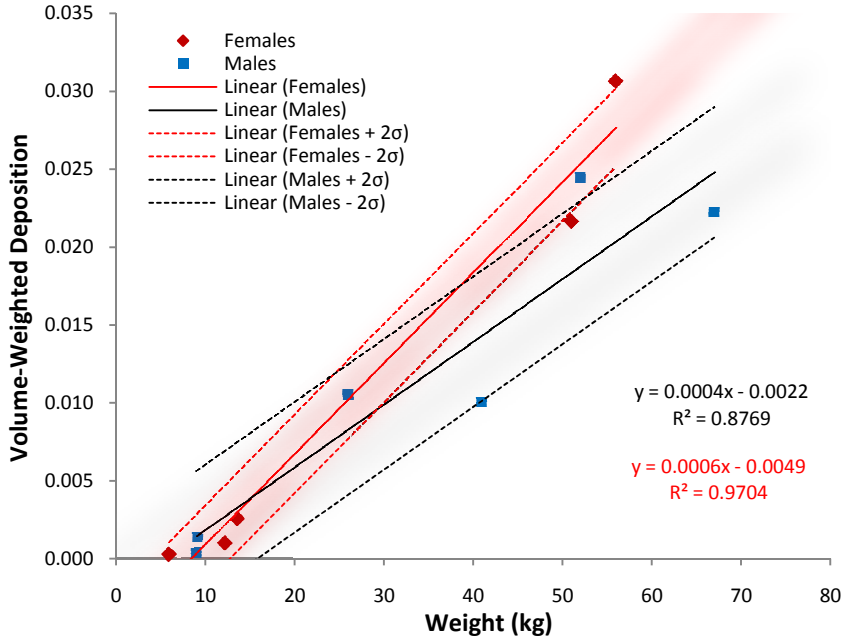

(b) Volume-weighted AL deposition as a function of weight

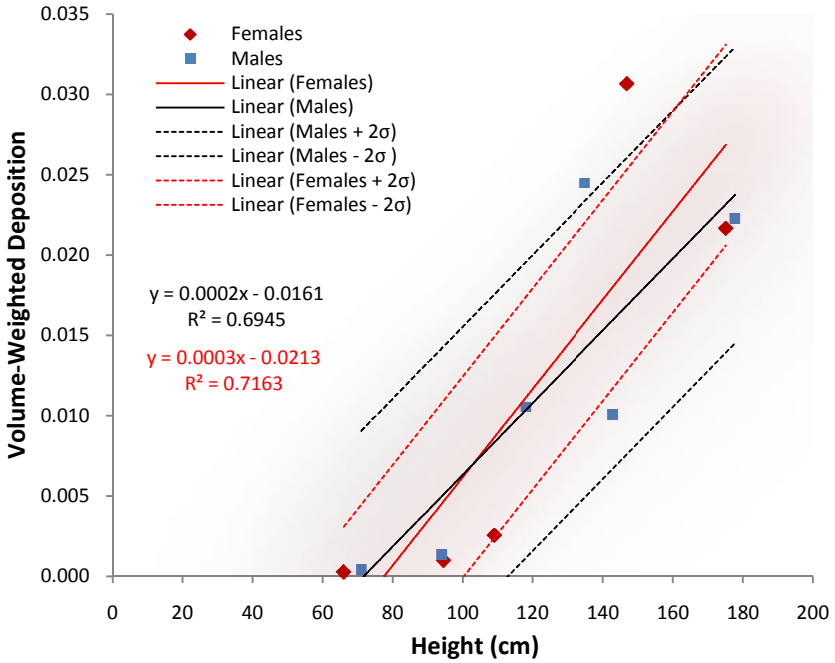

Figure 4: **(a)** Volume-weighted AL deposition as a function of height

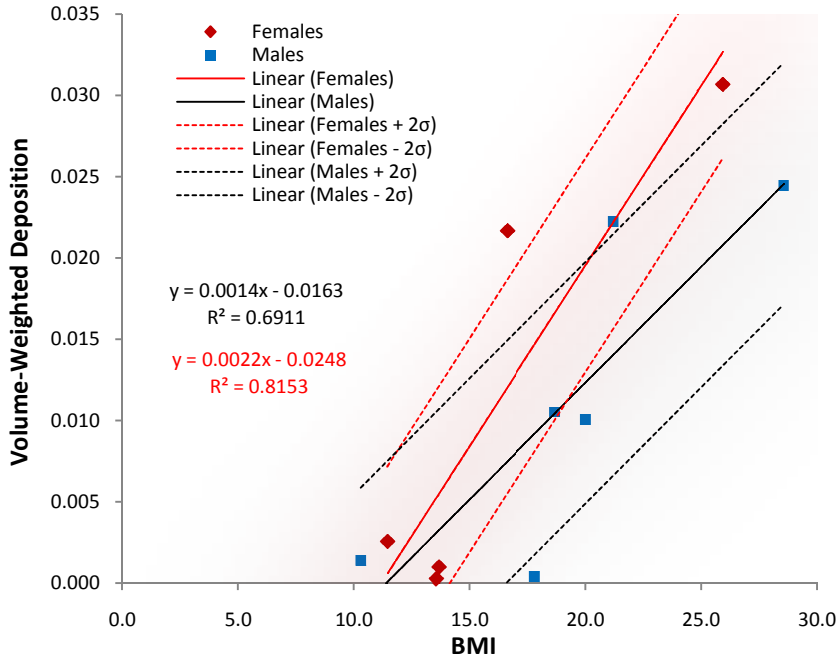

(b) Volume-weighted AL deposition as a function of BMI

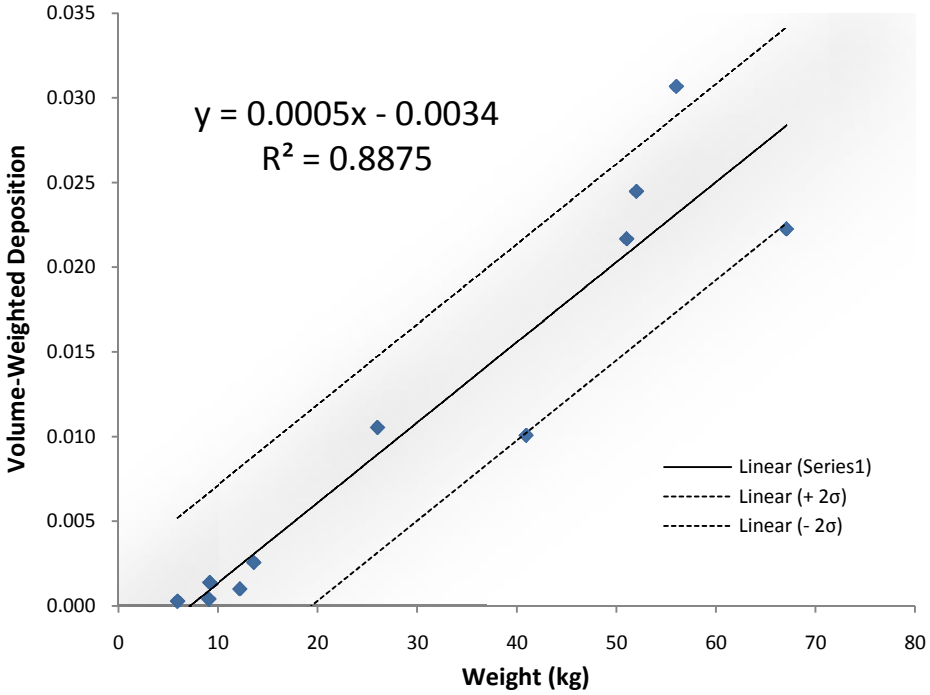

Figure 5: Volume-weighted AL deposition as a function of weight (genders combined)

Figures 6 (a) and (b) show the relationships between age and weight, respectively, and the optimal particle size where maximum volume-weighted deposition occurs. Figures 7 (a) and (b) show the relationships between height and BMI, respectively, and optimal particle size. It is apparent from these results that age and weight have stronger correlations to optimal particle size when compared to BMI. This is consistent with the results for volume-weighted deposition. This is evident by the larger scatter in the BMI data, drastically lower r^2 values, and considerably more broad 2σ limits.

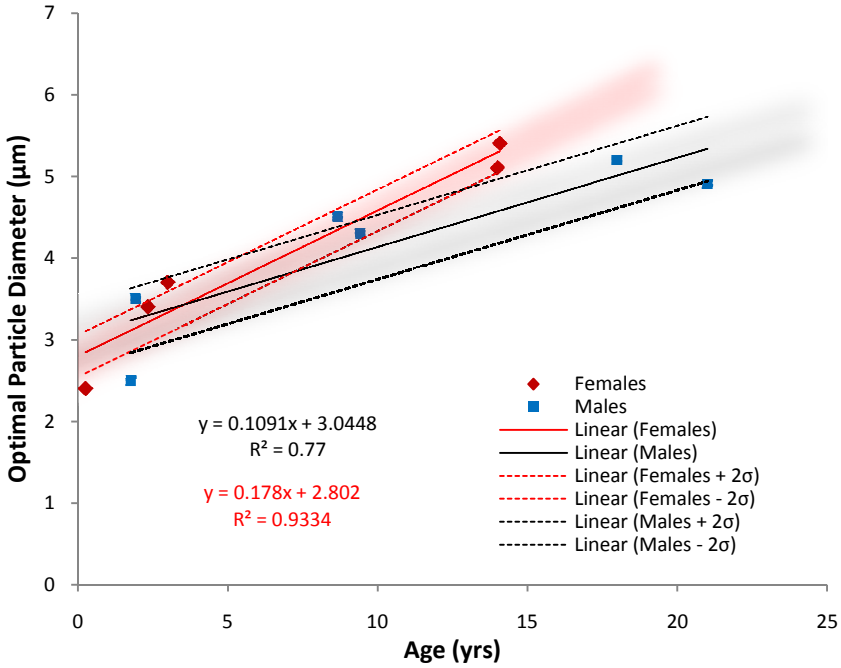

Figure 6: (a) Optimal particle size as a function of age

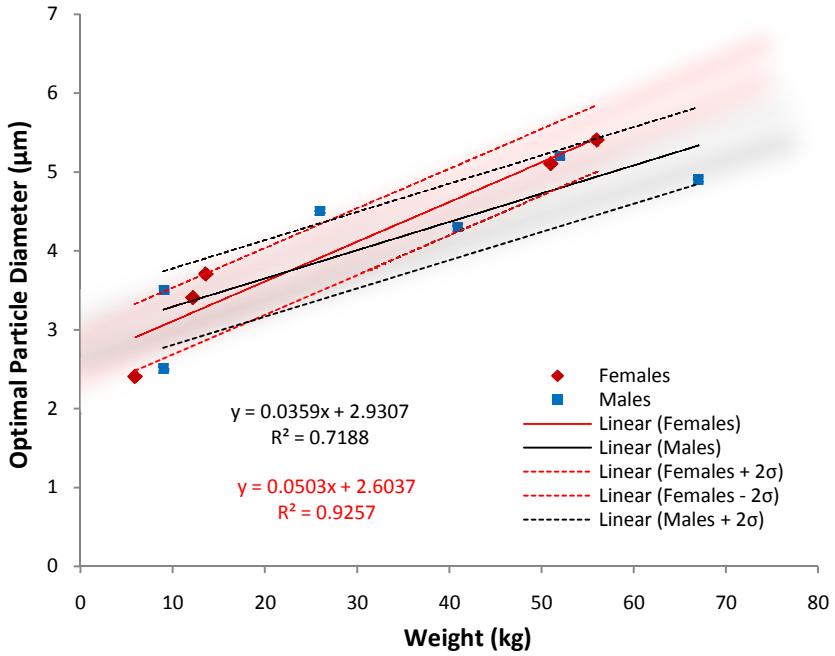

(b) Optimal particle size as a function of weight

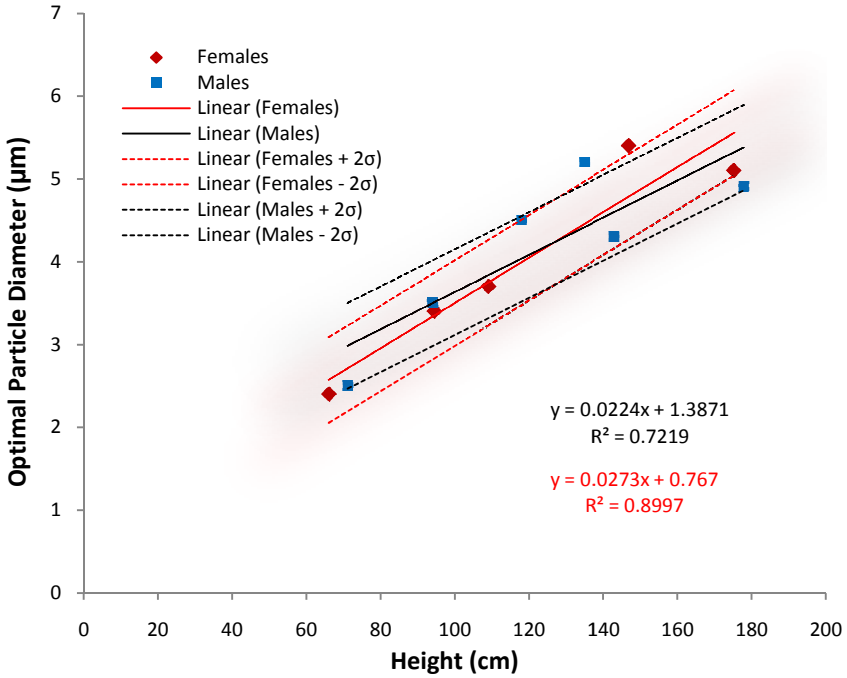

Figure 7: **(a)** Optimal particle size as a function of height

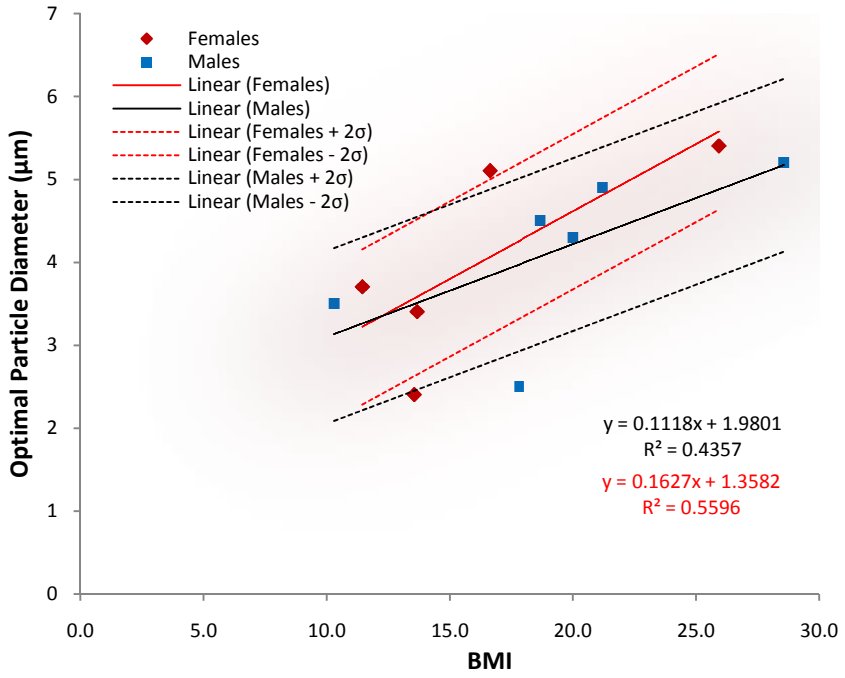

(b) Optimal particle size as a function of BMI

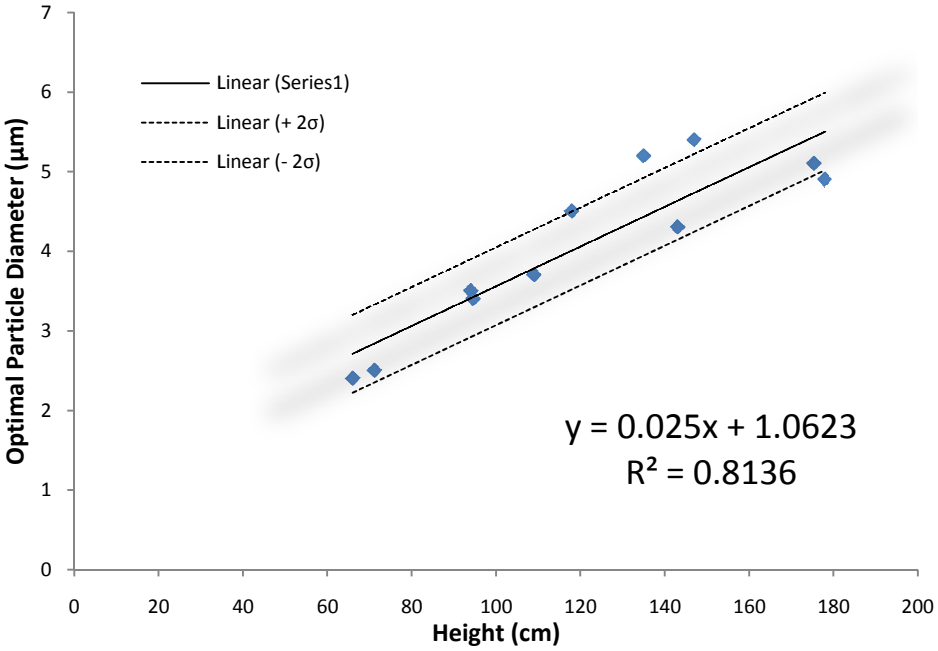

Figure 8: Optimal particle size for volume-weighted AL deposition as a function of height (genders combined)

Unlike the results for volume-weighted deposition, height also appears to have a similar relationship to optimal particle size as age and weight, which is seen in Figure 7 (a). Since there is virtually no difference between the results for males and females, the two genders are combined and displayed in Figure 8. The two points that lie above the 2σ bounds are for the 14.08-yr old female and 18-yr old male, both of which are considered abnormally short for their age. This may explain why they do not fall within the 2σ bounds when comparing optimal particle size to height.

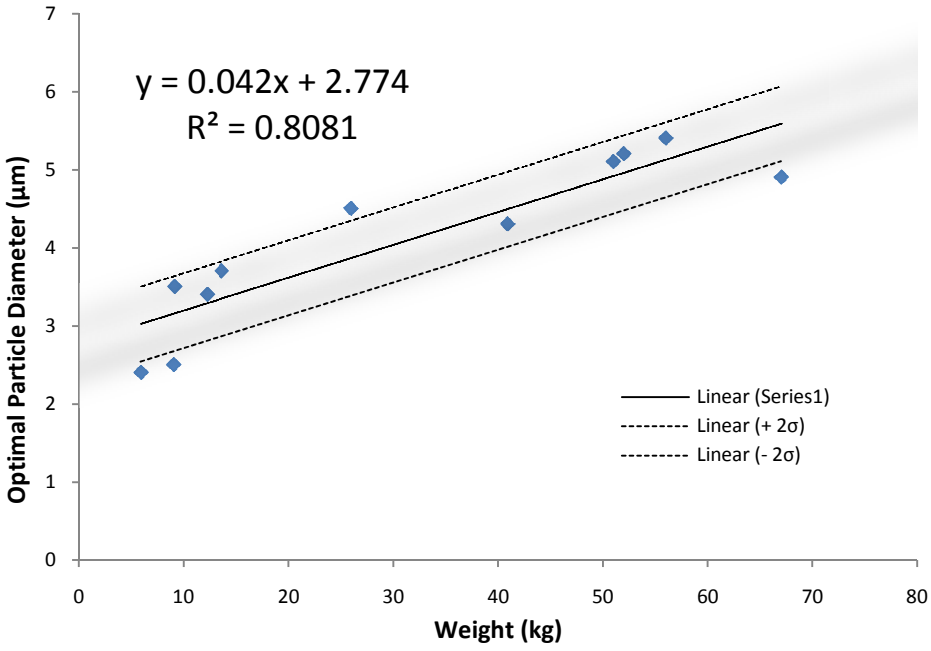

Figure 9: Optimal particle size for volume-weighted AL deposition as a function of weight (genders combined)

Figure 6 (b) also shows minimal difference between males and females in optimal particle size in relation to body weight. For optimal particle size, it is once again possible to develop a relationship as a function of body weight for humans in general and genders are combined. Figure 9 demonstrates this relationship; again notice that the majority of subjects in this study fall within 2σ of this relationship despite their gender. Based on these results, the following correlations can be used to determine volume-weighted deposition and optimal particle diameter for a subject of a particular weight:

$$d_{optimal}\ (\mu m) = 0.042 \cdot W\ (kg) + 2.774 \qquad (23)$$

$$VWD = 0.0005 \cdot W\ (kg) - 0.0034 \qquad (24)$$

where $d_{optimal}$ is the optimal particle diameter in μm, *VWD* is volume-weighted deposition, and *W* is body weight in kg.

3.32 Monodisperse vs. Polydisperse Sprays: Deposition and Optimal Particle Size Results

Based on the analysis, clear differences in deposition as a function of age are apparent. Figures 10 (a) and (b) compare the traditional particle deposition efficiency value based purely on number to the volume-weighted particle deposition in the alveolar region for children (under 10 years old). The lines on these figures are approximately where the maximum deposition occurs and assist in visually representing the shift, if one exists, in optimal particle size as age increases. Traditional deposition efficiency η (in %) is

$$\eta = \frac{N_{Gen}}{N_{Tot}} \qquad (25)$$

where N_{Gen} is the number of particles that deposit in a particular generation and N_{Tot} is the total number of particles. The traditional deposition efficiency describes a monodisperse spray well. Traditional deposition efficiency, calculated solely on the number of particles deposited, assumes that within a given tidal volume the same drug volume is delivered regardless of the particle size. In reality, however, particle size is a critical factor when determining delivered therapeutic dose. This is because the volume of a particle is proportional to the particle radius cubed and as a result the volume of therapeutic delivered is dependent upon the particle diameter (Newhouse and Ruffin 1979). For example, the particle number density in a monodisperse aerosol with 1 μm particles would need to be increased by a factor of 125 to achieve the same drug volume as a monodisperse aerosol with

5 μm particles because the radius of a 5 μm particle is 5 times greater than the radius of a 1 μm particle. There is some clinical evidence using monodisperse sprays that optimal alveolar deposition is obtained with particle diameters between 2 and 3 μm (Malcolmson and Embleton 1998), which is supported by Figure 10 (b). However, most aerosol devices used in a clinical setting deliver a polydisperse spray. Thus, should the optimal particle size be determined solely on the number of particles deposited or the largest volume deposited?

The volume-weighted deposition calculated in this study helps address this question. The volume-weighted deposition *VWD* is the traditional deposition efficiency multiplied by a particle volume weighting factor to take into consideration volume differences. It is nondimensional and is

$$VWD = \frac{N_{Gen}}{N_{Tot}} \frac{V_{PD}}{V_{10}} \qquad (26)$$

where V_{PD} is the volume of the particle being considered and V_{10} is the volume of the 10 micron particle. It assumes that the same particle number density is delivered, resulting in a greater therapeutic volume for larger particle diameters. For example, the volume-weighted deposition takes into consideration that, even if traditional deposition efficiency is higher for the 1 μm particle, the volume of therapeutic delivered per particle is 1000 times less than for the 10 μm. Notice the dramatic difference between the results. The traditional deposition efficiency based on number does not change substantially with age (this is true through adulthood and despite gender); however, the volume-weighted depositions and the particle sizes at which maximum volume-weighted deposition occurs are dependent upon age and body weight, which is evident in Figure 10 (a). Figure 10 (a) visually demonstrates that the

optimal particle size for volume-weighted deposition increases from 2.4 μm for the infant to 4.5 μm for the 9.42-yr old.

Finally, Figure 10 (a) is typical of later calculations that show that the volume of therapeutic delivered is dramatically different as age increases. At the optimal particle size for infants (2.4 μm) based upon volume-weighted deposition, the infant receives approximately 16 times less volume than the 8.67-yr old.

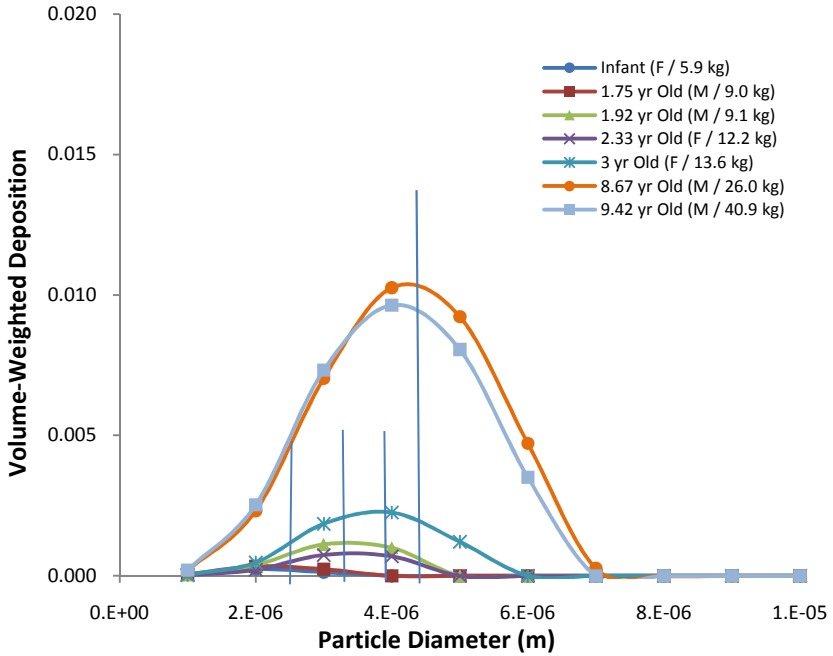

Figure 10: **(a)** Volume-weighted AL deposition for children under 10 years old

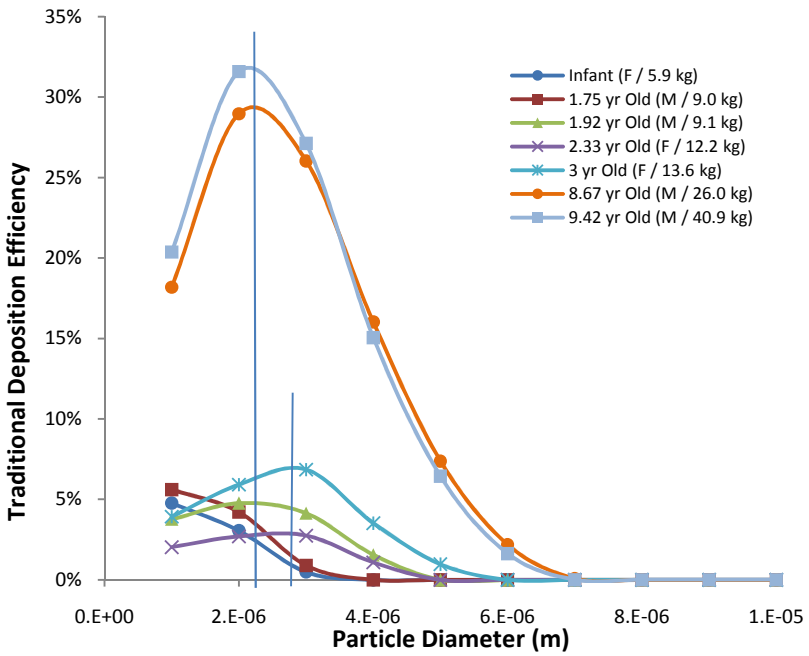

(b) Traditional AL deposition efficiency for children under 10 years old

Figures 11 (a) and (b) show the traditional deposition efficiency in the AL region for females and males, respectively. The maximum traditional deposition efficiency results and the particle diameters at which these maximum values occur are summarized in Table 5. Like the results for the children under 10 years old, the optimal particle size remains constant at approximately 2-3 μm. This is visually shown in Figures 11 (a) and (b), as well as seen in Table 5. In addition, these figures and this table show that the traditional deposition efficiency magnitude typically increases as age and body weight increase.

Figures 12 (a) and (b) show the volume-weighted deposition for the AL region. As age and body weight increase, AL volume-weighted deposition also consistently increases. It is apparent that the optimal particle size for deposition in the AL region of the lung increases as age and body weight increase as well, which is also evident in Figures 6 (a) and (b). The maximum volume-weighted deposition values, as well as the particle diameters at which these maximum values occur (optimal particle sizes), are summarized in Table 5.

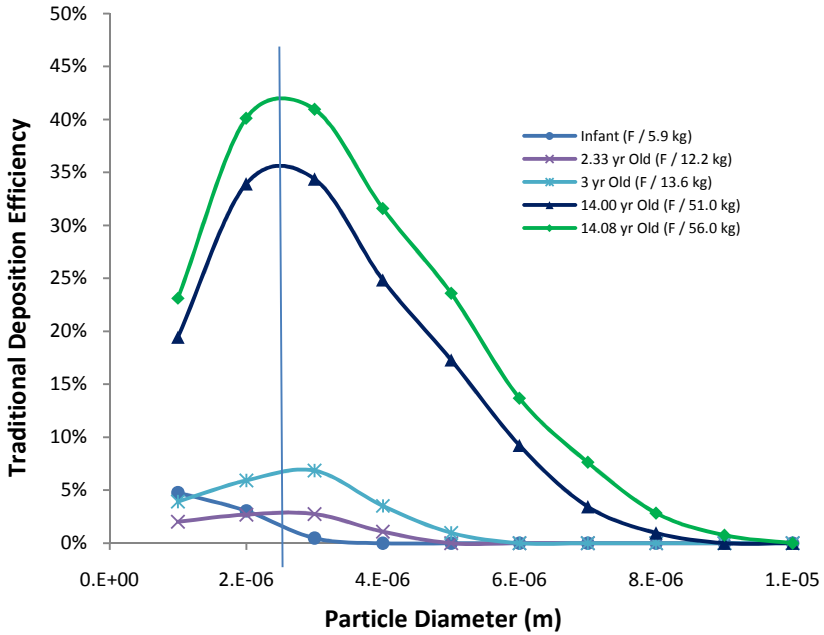

Figure 11: **(a)** Traditional AL deposition efficiency for females

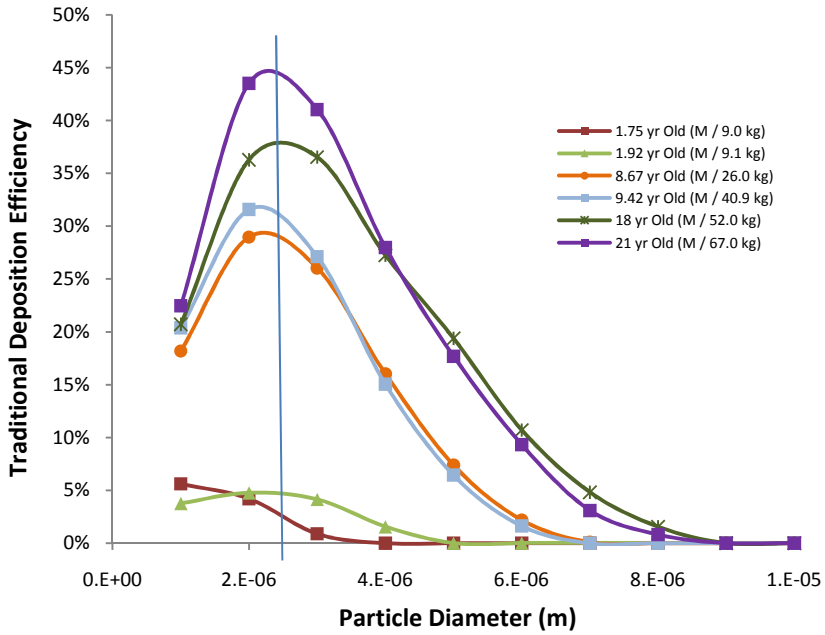

(b) Traditional AL deposition efficiency for males

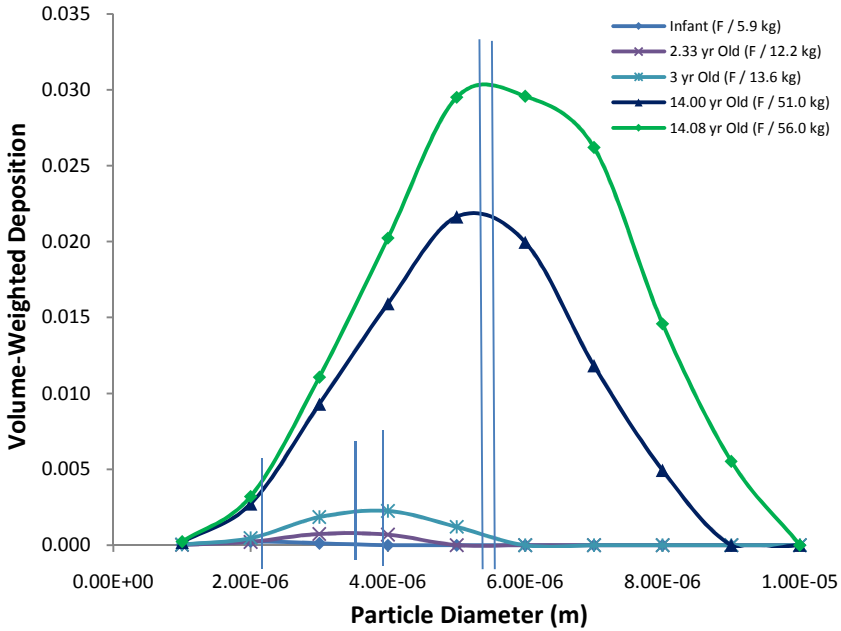

Figure 12: (a) Volume-weighted AL deposition for females

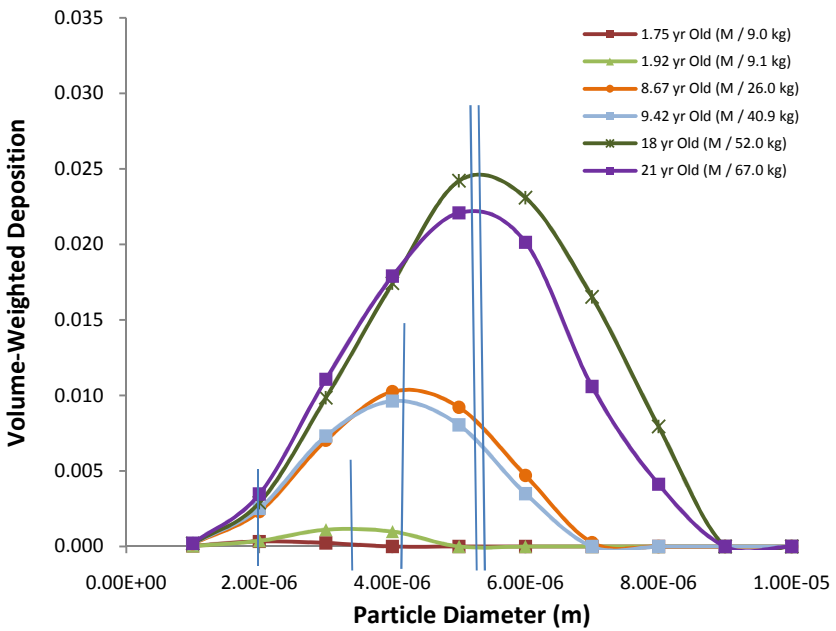

(b) Volume-weighted AL deposition for males

Table 5: Summary of results with exclusively humans: maximum volume-weighted deposition values, maximum traditional deposition efficiency values, and the particle diameters at which these maximum values occur

Age (yr)	Gender	Weight (kg)	Volume-Weighted Depositon	Optimal Particle Diameter (μm)	Traditional Deposition Efficiency	Optimal Particle Diameter (μm)
0.25	F	5.9	0.00026	2.4	4.78%	<1
1.75	M	9.0	0.00038	2.5	1.96%	<1
1.92	M	9.1	0.00136	3.5	4.98%	2.3
2.33	F	12.2	0.00097	3.4	2.94%	2.5
3.00	F	13.6	0.0025	3.7	6.90%	2.7
8.67	M	26.0	0.0105	4.5	30.06%	2.3
9.42	M	40.9	0.0100	4.3	32.04%	2.2
14.00	F	51.0	0.0216	5.1	35.96%	2.4
14.08	F	56.0	0.0306	5.4	42.50%	2.4
18.00	M	52.0	0.0244	5.2	38.75%	2.4
21.00	M	67.0	0.0222	4.9	43.82%	2.1

As seen in Table 5, these results show that the particle diameter should be adjusted for the appropriate age/body weight in order to maximize deposition in the desired region of the lung. These results also show that if a therapeutic that is designed for AL deposition in the adult is given to an infant, nearly all of the therapeutic will not reach the infant's alveolar region because the particle size is too large. The differences in deposition and optimal particle size as a function of age and body weight are expected because of the differences in lung size.

3.33 Breathing Rate Variation

All previous calculations were conducted at normal breath rates, but clinical studies suggest that there may be an optimal breath rate. To explore this concept, differences in breathing rates for three males (1.92-yr old, 9.42-yr old, and 21-yr old) are analyzed in this

study by varying breathing frequency. Figure 13 shows the traditional deposition efficiency as a function of breathing rate.

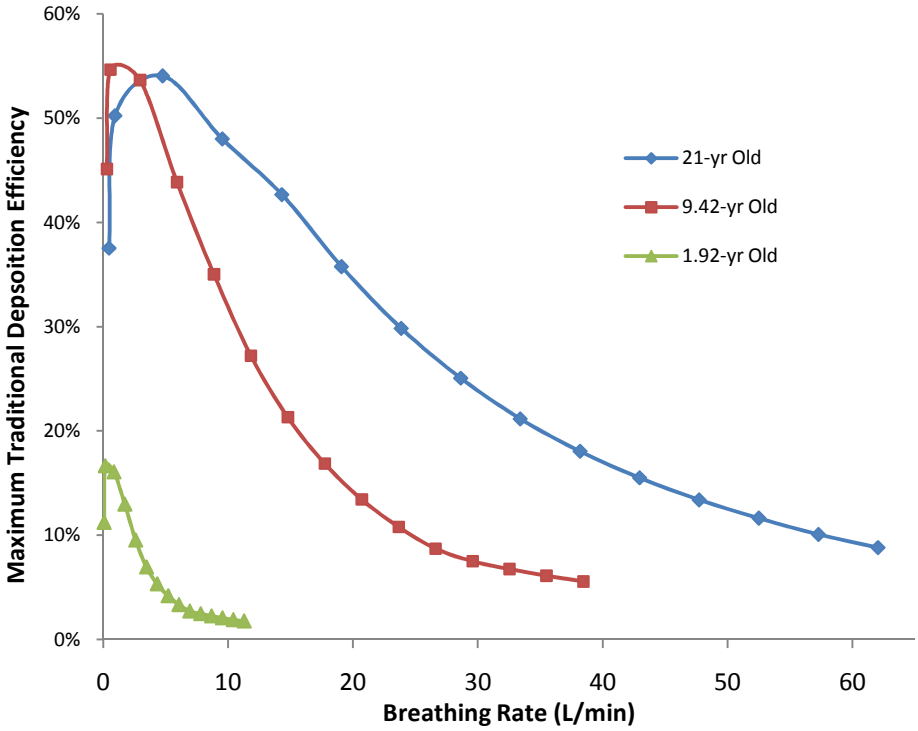

Figure 13: Maximum traditional deposition efficiency that occurs at each breathing rate

It is apparent from this figure that very low breathing rates are necessary for optimal traditional deposition efficiency. The particle sizes at which these optimal efficiency values occur are between 1 and 2 μm for all three ages. Moreover, the breathing rates at which optimal deposition efficiency occurs are considerably lower than normal tidal breathing rates for all of the subjects represented.

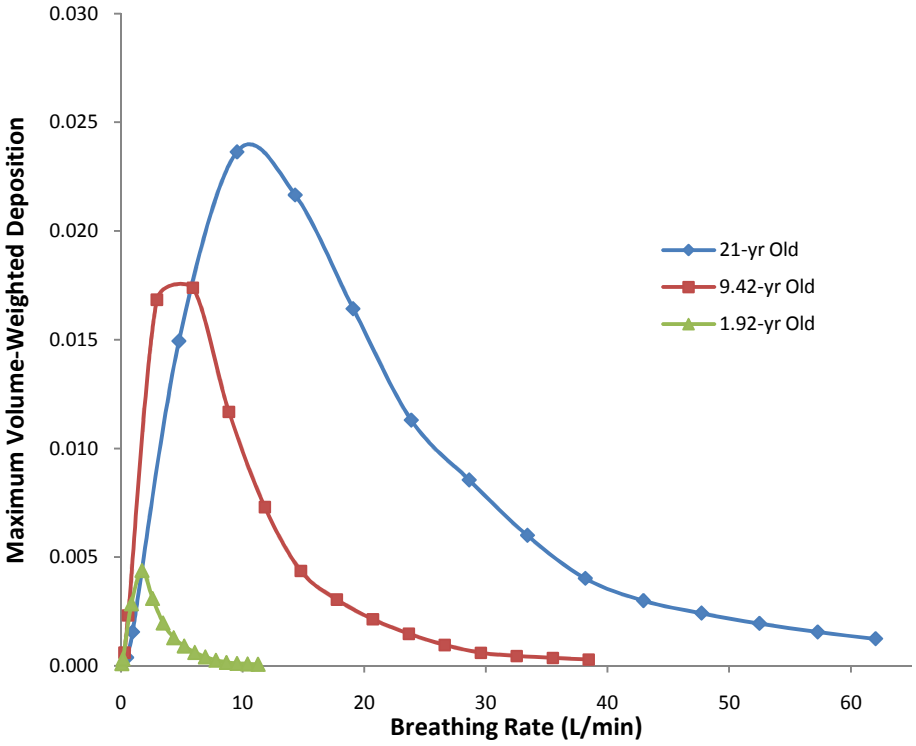

Figure 14: Maximum volume-weighted deposition that occurs at each breathing rate

Figure 14 shows the maximum volume-weighted deposition that occurs at each breathing rate. This figure clearly shows that different breathing rates are necessary for each age for optimal deposition, as well as verifies that maximum volume-weighted deposition is age and body weight dependent. Table 6 shows the maximum volume-weighted deposition values in addition to the particle sizes and breathing rates at which these maximums occur. Table 7 shows the maximum volume-weighted deposition and the corresponding particle sizes at normal breathing rates.

Table 6: Maximum volume-weighted deposition and the breathing rates where the maximum values occur

Age (yr)	Weight (kg)	Maximum Volume-Weighted Deposition	Breathing Rate (L/min)	Particle Diameter (μm)
1.92	9.1	0.0046	1.39	4.1
9.42	40.9	0.0206	4.14	5.0
21.00	67	0.0243	9.54	5.3

Table 7: Maximum volume-weighted deposition at normal breathing rates

Age (yr)	Weight (kg)	Maximum Volume-Weighted Deposition	Normal Breathing Rate (L/min)	Particle Diameter (μm)
1.92	9.1	0.0014	4.72	3.5
9.42	40.9	0.0100	10.09	4.3
21.00	67	0.0222	13.73	4.9

Based on these results, the breathing rate at which maximum volume-weighted deposition occurs is different for all three ages. In addition, for all of the ages, the breathing rates at which the maximum volume-weighted deposition occurs are lower than normal tidal breathing rates. Controlling breathing rates can be very difficult for younger ages and it possibly not feasible; nevertheless, based on these results deposition can be improved if the older children and adults can control breathing rate, which is likely achievable. Comparison of Tables 6 and 7 shows that for the 1.92-yr old, the volume-weighted deposition that occurs at the optimal breathing rate is approximately 3.3 times higher than that which occurs at the normal breathing rate. Also, the optimal breathing rate is approximately 3.4 times less than the normal breathing rate for this age. For the 9.42-yr old, the volume-weighted deposition at the optimal breathing rate for this age is nearly twice that which occurs at the normal breathing rate. For this age, the optimal breathing rate is almost 2.5 times the normal breathing rate. For the 21-yr old, the volume-weighted deposition at the optimal breathing rate is only approximately one tenth higher than the deposition that occurs at the normal

breathing rate, and the optimal breathing rate is only approximately four tenths higher than the normal breathing rate. Based on these results, the optimal breathing rates get closer to normal breathing rates as age/body weight increase. Also, lowering the breathing rate to maximize deposition is more important for children than for adults based on the difference in magnitude of volume-weighted deposition at optimal and normal breathing rates. Tables 6 and 7 also show that at the optimal breathing rates, the optimal particle size is nearly half a micron higher than at normal breathing rates. This essentially means that optimal particle size is dependent upon breathing rate.

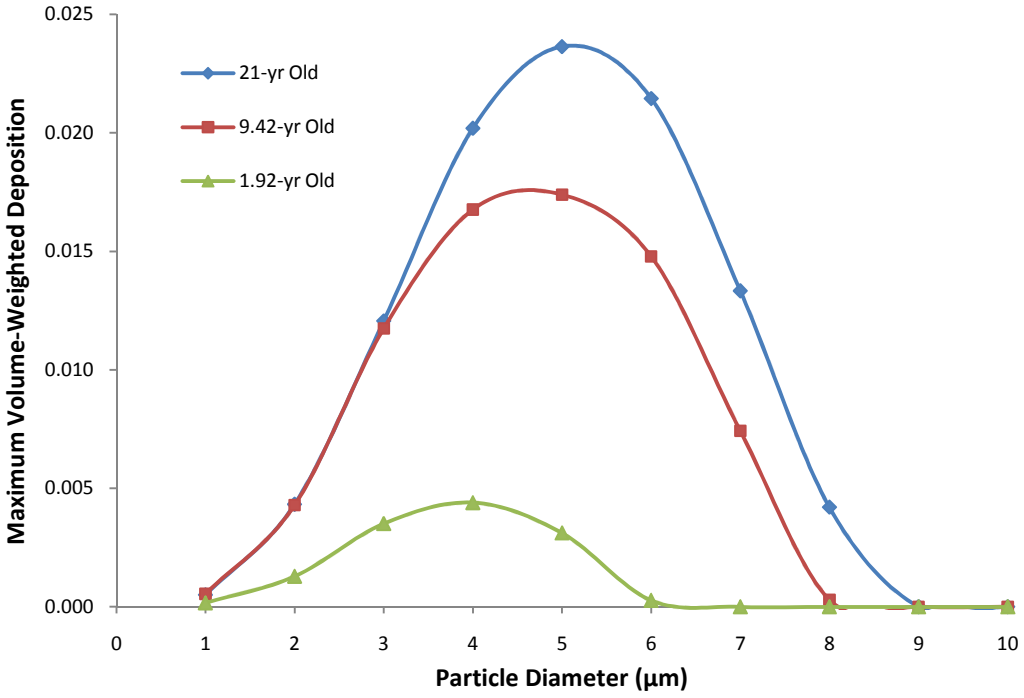

Figure 15: Particle size where maximum volume-weighted deposition occurs

Figure 15 verifies that even when at the optimal breathing rates for each age, the magnitude of maximum volume-weighted deposition and the optimal particle size are age and body weight dependent. It is also significant to mention that tidal breathing rates vary throughout the population and that these variations will affect deposition results.

3.34 Sensitivity Analysis

Sensitivity is determined for volume-weighted deposition as a function of breathing rate and particle diameter by evaluating the change in the performance parameter, normalized, to the change in the input variable, normalized. For example, when performing the sensitivity of volume-weighted deposition to breathing rate, the performance parameter is the volume-weighted deposition and the input variable is the breathing rate. The larger the sensitivity value, the more sensitive the performance parameter is to the input variable.

The sensitivity analyses for the 1.92-yr old as a function of breathing rate and particle diameter are given in Tables 8 (a) and (b), respectively. Tables 9 (a) and (b) show the sensitivity analyses for the 9.42-yr old, and Tables 10 (a) and (b) show the sensitivity analyses for the 21-yr old. The values highlighted in green are the normal tidal breathing rates for each age and the values highlighted in blue are the optimal breathing rates, which were determined when evaluating the effect of breathing rate on deposition. The values shown in red are where the maximum volume-weighted deposition values occur.

1.92-yr Old	Particle Diameter (µm)									
Breathing Rate (L/min)	1	2	3	4	5	6	7	8	9	10
0.087										
0.17	0.652	2.000								
0.87	-0.606	0.931	1.250	1.250	1.250					
1.39	-0.522	-0.202	0.488	**0.779**	1.509					
1.74	-0.437	-0.409	-0.236	-0.142	-0.032	3.000				
2.60	-1.265	-1.538	-1.450	-1.660	-2.369					
3.47	-0.888	-1.284	-1.404	-2.142	-4.640					
4.72	-2.941	-4.895	**-7.347**	**-10.708**						
5.21	-0.569	-0.979	-1.464	-2.801						
6.07	-2.173	-4.378	-9.593	-40.256						
6.94	-0.968	-2.036	-5.243	-357.199						
7.81	-0.978	-2.195	-6.121							
8.68	-0.989	-2.376	-5.156							
9.54	-1.001	-2.587	-7.315							
10.41	-1.012	-2.841	-12.174							

1.92-yr Old	Particle Diameter (µm)									
Breathing Rate (L/min)	1	2	3	4	5	6	7	8	9	10
0.087										
0.17		0.985								
0.87		1.825	1.651	-0.075	-13.183					
1.39		1.847	2.074	**0.711**	-2.310					
1.74		1.849	2.121	0.806	-2.053	-62.899				
2.60		1.841	2.135	0.683	-2.938					
3.47		1.827	2.115	0.210	-6.294					
4.72		1.803	**1.977**	**-0.491**						
5.21		1.792	1.914	-1.201						
6.07		1.747	1.457	-10.266						
6.94		1.720	1.009	-362.784						
7.81		1.689	0.368							
8.68		1.653	-0.180							
9.54		1.611	-1.210							
10.41		1.560	-3.691							

Table 8: (a) Breathing rate sensitivity analysis for the 1.92-yr old (top)
(b) Particle diameter sensitivity analysis for the 1.92-yr old (bottom)

9.42-yr Old	Particle Diameter (µm)									
Breathing Rate (L/min)	1	2	3	4	5	6	7	8	9	10
0.30										
0.59	0.349	1.480	2.000							
2.96	-0.421	0.573	1.107	1.250	1.250	1.250	1.250			
4.14	-0.788	-0.437	-0.086	0.376	**0.639**	0.730	2.286			
8.87	-0.918	-0.678	-0.694	-1.059	-1.665	-2.587	-10.743			
10.09	-0.825	-0.901	-1.183	**-1.761**	**-2.939**	-6.658				
11.83	-0.909	-1.093	-1.489	-2.173	-5.032	-11.900				
14.79	-1.044	-1.386	-1.971	-3.371	-7.521					
17.75	-1.083	-1.581	-2.478	-4.790	-21.309					
20.71	-1.115	-1.793	-2.977	-7.223	-41.328					
23.67	-1.144	-1.956	-3.603	-10.315						
26.62	-2.393	-4.793	-13.156	-55.236						
29.58	-1.116	-2.374	-5.718	-28.834						
32.54	-1.152	-2.653	-5.251							
35.50	-1.186	-3.017	-6.870							

9.42-yr Old	Particle Diameter (µm)									
Breathing Rate (L/min)	1	2	3	4	5	6	7	8	9	10
0.30		0.508								
0.59		1.530	-2.177							
2.96		1.809	1.904	1.120	0.156	-2.479	-19.123			
4.14		1.825	2.002	1.491	**0.563**	-2.208	-4.447			
8.87		1.840	1.996	1.135	-0.353	-4.345	-25.376			
10.09		1.839	1.965	**0.960**	**-0.981**	-7.775				
11.83		1.835	1.913	0.709	-2.886	-15.769				
14.79		1.826	1.813	0.048	-6.795					
17.75		1.813	1.673	-1.030	-24.852					
20.71		1.798	1.494	-3.170	-96.433					
23.67		1.780	1.245	-7.318						
26.62		1.733	0.181	-28.815						
29.58		1.703	-0.581	-77.074						
32.54		1.666	-1.263							
35.50		1.620	-2.356							

Table 9: **(a)** Breathing rate sensitivity analysis for the 9.42-yr old (top)
(b) Particle diameter sensitivity analysis for the 9.42-yr old (bottom)

21-yr Old	Particle Diameter (µm)									
Breathing Rate (L/min)	1	2	3	4	5	6	7	8	9	10
0.48										
0.95	0.506	1.831	2.000							
4.77	-0.132	0.800	1.238	1.250	1.250	1.250				
9.54	-1.048	-0.252	0.247	0.521	**0.997**	**1.421**	2.000	2.000		
13.73	-1.071	-0.339	-0.290	-0.418	**-0.229**	-0.213	-0.844	-0.054		
19.09	-1.142	-0.772	-0.868	-0.942	-1.231	-2.344	-4.575			
23.86	-1.091	-0.992	-1.248	-1.266	-2.487	-4.691	-13.748			
28.63	-1.082	-1.144	-1.319	-1.936	-3.945	-10.018				
33.40	-1.076	-1.293	-1.668	-2.975	-6.478	-18.163				
38.18	-1.072	-1.378	-2.122	-3.935	-6.974					
42.95	-1.070	-1.477	-2.182	-4.079	-9.871					
47.72	-1.069	-1.572	-2.410	-4.544	-21.010					
52.49	-1.069	-1.667	-2.671	-5.529	-21.559					
57.26	-1.070	-1.846	-2.969	-7.798						
62.03	-1.071	-1.874	-3.308	-9.654						

21-yr Old	Particle Diameter (µm)									
Breathing Rate (L/min)	1	2	3	4	5	6	7	8	9	10
0.48		-3.689								
0.95		1.355	-42.796							
4.77		1.790	1.773	1.169	-1.296	-5.457				
9.54		1.845	2.045	1.611	**0.729**	**-0.611**	-4.266	-17.402		
13.73		1.871	2.058	1.525	**0.947**	-0.580	-6.304	-12.533		
19.09		1.881	2.037	1.485	0.687	-2.108	-11.329			
23.86		1.883	1.995	1.478	-0.154	-4.494	-28.461			
28.63		1.882	1.971	1.265	-1.458	-10.902				
33.40		1.879	1.924	0.852	-3.727	-25.555				
38.18		1.875	1.839	0.288	-5.949					
42.95		1.870	1.761	-0.341	-10.798					
47.72		1.864	1.671	-1.088	-28.685					
52.49		1.857	1.566	-2.151	-61.353					
57.26		1.848	1.450	-4.135						
62.03		1.840	1.300	-7.301						

Table 10: (a) Breathing rate sensitivity analysis for the 21-yr old (top)
(b) Particle diameter sensitivity analysis for the 21-yr old (bottom)

Aside from the top row of the breathing rate sensitivity results and the 1 micron column for the particle diameter sensitivity results, all of the blank positions in each table are present because the volume-weighted deposition values are zero and consequently sensitivity calculations are not applicable.

Tables 8 (a) and (b) show that for young children, sensitivity to breathing rate is greater than sensitivity to particle diameter at normal breathing rates. However, the sensitivity of volume-weighted deposition to both breathing rate and particle diameter are the lowest at the optimal breathing rate. Tables 9 (a) and (b) show that for older children, the sensitivity of volume-weighted deposition to breathing rate is only slightly higher than sensitivity to particle diameter, exhibiting the lowest sensitivity to both at optimal breathing rates. Tables 10 (a) and (b) show that for healthy adults, the magnitude of sensitivity of volume-weighted deposition to both breathing rate and particle diameter is similar regardless of breathing rate. Also, there does not appear to be a difference in sensitivity at the normal breathing rate and optimal breathing rate. This is possibly because these two breathing rates are in close proximity to each other.

Also, when comparing Tables 8-10 (a), it is apparent that sensitivity to breathing rate changes as a function of age and/or body weight. The sensitivity is not the same for the 1.92-yr old as it is for the 21-yr old; at normal breathing rates, sensitivity of volume-weighted deposition to breathing rate decreases as age/ body weight increase. However, Tables 8-10 also show that at the optimal breathing rate and optimal particle diameters, the sensitivity to breathing rate and particle diameter tends to be relatively low for all ages.

3.4 Conclusions

For volume-weighted alveolar deposition, the variation of optimal particle size is ~2.5 μm for infants to 5-6 μm for adults. This represents a two-fold increase in optimal particle size as age/body weight increase. This study brings to light the correlations that exist for both genders between deposition and factors such as age and body weight. This is done for the purpose of developing relationships between age and weight to optimal particle size and volume-weighted deposition. For volume-weighted deposition and optimal particle diameter as a function of weight, significant overlap occurs between the two genders and the genders are combined. The following correlations can be used to determine approximate volume-weighted deposition *VWD* and optimal particle diameter $d_{optimal}$ at normal breathing rates for both genders of a particular weight *W*.

$$d_{optimal}\ (\mu m) = 0.042 \cdot W\ (kg) + 2.774$$

$$VWD = 0.0005 \cdot W\ (kg) - 0.0034$$

The results of this study indicate that slowing breathing rates below normal breathing rates, especially in children, will likely enhance deposition performance. Also, the results indicate that optimal particle size shifts as a result of changes in breathing rate and this should be taken into consideration when developing delivery devices and delivering therapeutics.

The sensitivity analysis performed shows that for very young children, sensitivity to changes in breathing rate is greater than sensitivity to changes in particle diameter at normal breathing rates. However, the sensitivity of volume-weighted deposition to both breathing rate and particle diameter are the lowest at the optimal breathing rate. For older children, the

sensitivity of volume-weighted deposition to breathing rate is only slightly higher than sensitivity to particle diameter, exhibiting the lowest sensitivity to both at optimal breathing rates. For healthy adults, the magnitude of sensitivity of volume-weighted deposition to both breathing rate and particle diameter is similar regardless of breathing rate, and there does not appear to be a difference in sensitivity at the normal and optimal breathing rates.

However, these results only take into account one morphometric model for each represented age. Since lung geometry can vary significantly between individuals, additional research is needed to address the differences between individuals of each age group as well as the differences between males and females of the same age and body weight. Additionally, more research is needed for adolescents and adults to determine if a relationship exists between BMI and optimal particle size or volume-weighted deposition since a limited number of subjects of these ages is presented in this study.

Further, these results fail to capture that differences exist in inspiration and expiration rates. Moreover, clinical studies are needed to validate these statistical results because the models used in this study are static and fail to account for the dilation of the lung geometry during inspiration and expiration. It is only in models that can capture this aspect that the effects of lung remodeling as a result of health status can be explored.

CHAPTER FOUR: COMPARISON BETWEEN HUMANS AND ANIMALS

4.1 Introduction

Particle deposition calculations are performed for a mouse, rat, and canine and compared to the human models. These animals vary in body size and weight and are frequently used in dosing studies; therefore, they are compared to humans to determine their applicability in relation to particle deposition for the various human ages presented in this study. Body weight is the only appropriate comparison parameter between humans and animals; therefore, body weight is used to evaluate deposition in animals and provide comparison with humans.

4.2 Methods

In the calculations with humans and animals, traditional deposition efficiency and volume-weighted deposition are once again determined for the alveolar region. However, as previously mentioned, respiratory bronchioles are not present in the mouse and rat, and thus only the conducting airways and the alveolar region are specified. As a result, to allow for more accurate comparison, the generations included in the alveolar region of the lung are modified for the human models so that the alveolar region is described in a similar fashion to the animal models. In the human models, the terminal bronchiole and respiratory bronchiole generations are considered to be part of the alveolar region when compared with the animal species. Consequently, for the infants and young children (3-mo old to 3-yr old), generations

15-23 are considered to be the alveolar region. For the other ages that are evaluated (8.67-yr old to 21-yr old), generations 15-24 are considered to be the alveolar region. However, generation 24 is once again not included in the deposition calculations for the 21-yr old because the tidal volume will not reach this generation, as discussed in Chapter 3.

The total number of generations in the lung and the number of generations in the alveolar region are dependent upon the animal species. For the mouse, generations 15-21 make up the alveolar region. For the rat, generations 15-23 are considered to be the alveolar region. For the canine, the alveolar region consists of generations 21-29.

4.3 Results and Discussion

Figure 16 (a) shows the volume-weighted deposition for humans and animals. Figure 16 (b) shows the optimal particle size for volume-weighted deposition for humans and animals. Based on Figure 16 (a), the rate at which deposition increases as a function of body weight is only slightly higher for animals than for humans, but the difference in magnitude of deposition as a function of body weight in animals and humans appears to be statistically significant. For example, the magnitude of volume-weighted deposition for the mouse appears to be nearly equal to that of the 3-yr old despite a considerable difference in body weight.

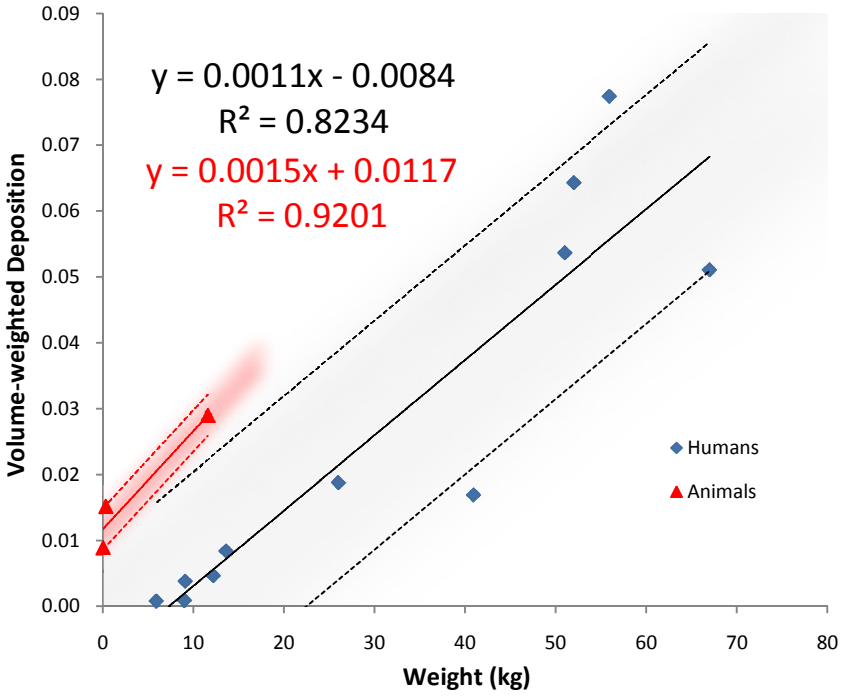

Figure 16: (a) VWD as a function of weight (humans and animals)

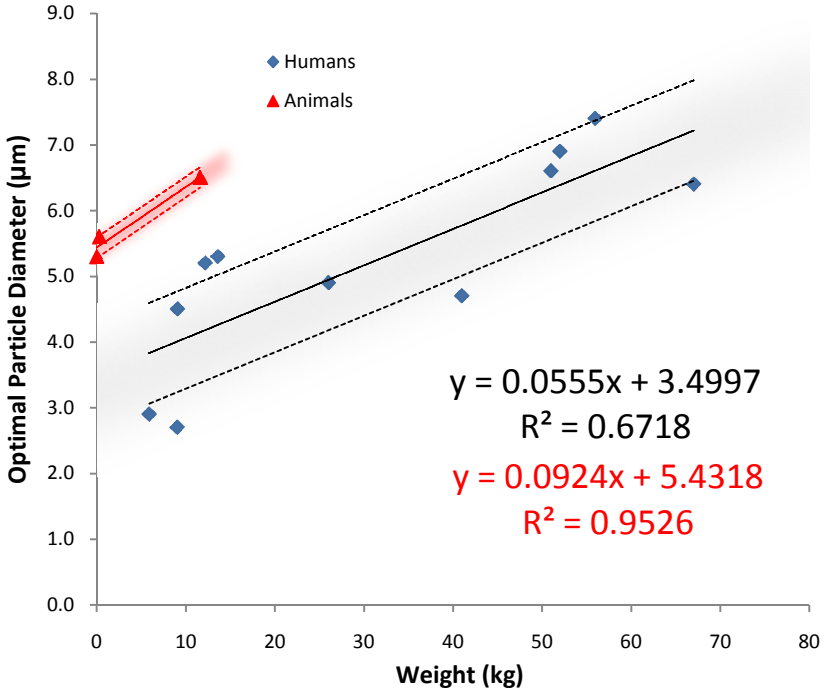

(b) Optimal particle size for VWD as a function of weight (humans and animals)

Figure 16 (b) shows that the rate at which optimal particle diameter for volume-weighted deposition increases in relation to body weight is higher for animals that for humans; the rate of increase in optimal particle size for volume-weighted deposition is 2/3 times higher for animals than for humans. In addition, there is once again a difference between humans and animals in relation to optimal particle size magnitude; the magnitude of optimal particle size for volume-weighted deposition in relation to body weight is higher for animals than for humans.

The human and animal results for traditional deposition efficiency, volume-weighted deposition, and optimal particle sizes for each are summarized in Table 11. Despite redefining the alveolar region for the humans, the optimal particle size for traditional deposition efficiency remains relatively constant between 2.5 to 4 μm for all species regardless of body weight.

Table 11: Summary of results with animals and humans: maximum volume-weighted deposition values, maximum traditional deposition efficiency values, and the particle diameters at which these maximum values occur

Age (yr)	Gender	Weight (kg)	Volume-Weighted Depositon	Optimal Particle Diameter (μm)	Traditional Deposition Efficiency	Optimal Particle Diameter (μm)
0.25	F	5.9	0.00072	2.9	6.87%	<1
1.75	M	9.0	0.00081	2.7	7.57%	<1
1.92	M	9.1	0.00373	4.5	7.94%	2.5
2.33	F	12.2	0.00456	5.2	6.59%	3.5
3.00	F	13.6	0.00831	5.3	11.38%	3.5
8.67	M	26.0	0.01869	4.9	34.67%	2.4
9.42	M	40.9	0.01682	4.7	36.39%	2.3
14.00	F	51.0	0.05358	6.6	44.72%	3.3
14.08	F	56.0	0.07735	7.4	51.22%	3.3
18.00	M	52.0	0.06423	6.9	47.69%	3.2
21.00	M	67.0	0.05099	6.4	51.57%	3
$B6C3F_1$ Mouse		0.0256	0.00887	5.3	10.81%	3.7
Long- Evans Rat		0.33	0.01512	5.6	15.95%	3.7
Beagle Dog		11.6	0.02891	6.5	26.88%	3.2

When considering the animal results, the alveolar deposition and optimal particle sizes for the animals increase as a result of body size increase (from mouse to rat to canine). However, even though the mouse is considerably smaller in size than all of the humans, Table 11 shows that the volume-weighted deposition and traditional deposition efficiency for the mouse very closely correspond to that of the 3-yr old, as well as the optimal particle size for volume-weighted deposition. The volume-weighted deposition and traditional deposition efficiency values for the other animal species increase from here.

These results are also displayed in Figure 17, which shows volume-weighted deposition as a function of particle diameter for the animal species in comparison with humans. The similarities between animals and humans are surprising given the dramatic difference in airway dimensions, particularly from a mouse to an adult human. For example, the diameter and length of the mouse trachea are 0.137 cm and 0.897 cm, respectively, whereas the diameter and length of the 21-yr old human trachea are 2.060 cm and 12.920 cm, respectively. Clearly, from these dimensions alone it is apparent that the difference between the airway dimensions and the resulting airway volumes of these species is quite significant. Also, it is surprising to observe that the smallest animal exhibits optimal particle sizes within a range consistent with the younger humans.

Comparison of Table 5 and Table 11 shows that the optimal particle size for humans has shifted higher for each age as a result of adding the respiratory bronchioles to the alveolar region. These results are anticipated because the optimal particle size for volume-weighted deposition in the respiratory bronchioles was calculated to be approximately 2 μm higher for a particular age than the alveolar deposition. Additionally, the magnitude of

volume-weighted deposition for the humans increases as a result of adding the respiratory bronchioles to the alveolar region, but these results are expected.

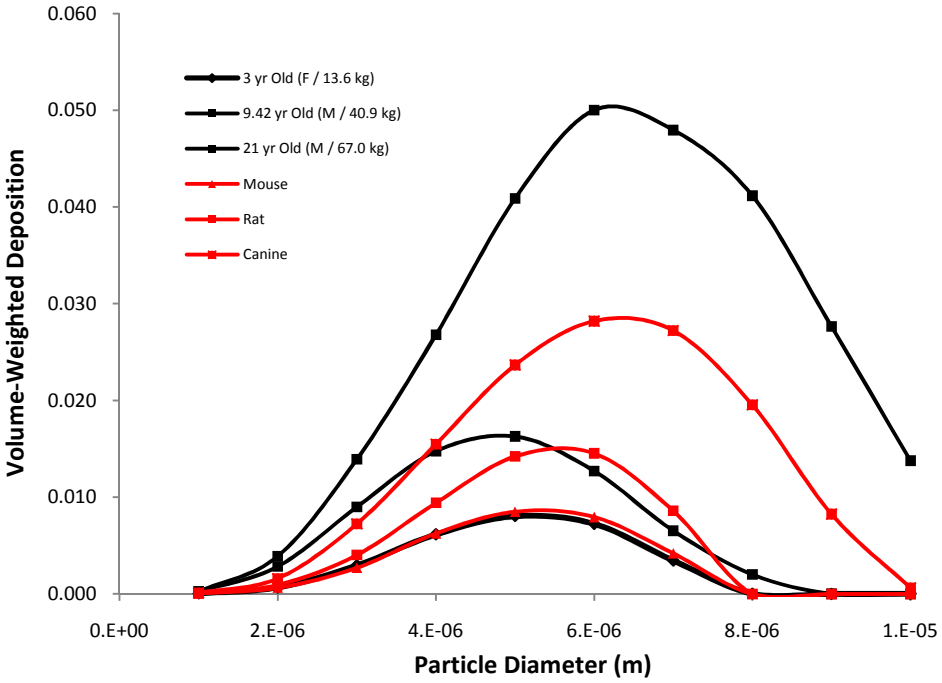

Figure 17: Volume-weighted AL deposition in humans and animals

Based on Figure 17, the mouse deposition and optimal particle size correspond closely with the 3-yr old and as a result the mouse is a generally a relatively good model for infants and young children. Despite a slight difference in optimal particle size, the similarities in volume-weighted deposition between the rat and the 9.42-yr old indicate that the rat is likely a relatively good model for older children. Also, even though the deposition in the canine does not correspond to any of the particular human subjects presented in this

study, the volume-weighted deposition and optimal particle size indicate that the canine likely represents adolescents reasonably well.

4.4 Conclusions

Having a firm understanding of the changes in deposition between animal models and the human target population is critical when translating dosing level from an animal model to a human model. Simply administering more drug for a higher body mass is likely inappropriate and could potentially lead to over or under dosing.

These results indicate that the mouse represents the traditional deposition efficiency, volume-weighted deposition, and optimal particle size for the 3-yr old female very well and is likely generally a good model of optimal particle size for younger children. The rat is likely a good model for older children based on the similarities in volume-weighted deposition to the 9.42-yr old. The canine, on the other hand, likely models adolescent humans reasonably well generally although it does not exactly match any of the subjects presented in this study. The rates of increase of deposition and optimal particle size as a function of mass, however, are different among the animals and the small human sample population represented in this study.

Furthermore, it is obvious from the increase in volume-weighted deposition and the shift in optimal particle size that that deposition and optimal particle sizes for humans depend upon how the regions of the lung are defined. If the generations that are included in the alveolar region are changed, these results demonstrate that the deposition will change. Awareness of this is critical when determining and comparing deposition between various

models. It is important to define similar lung regions for each model for the results to be accurately compared.

CHAPTER FIVE: HELIOX COMPARED TO AIR

5.1 Introduction and Methods

Calculations for the humans and animals are performed with 80/20 heliox in addition to air because some research studies suggest that heliox decreases resistance in the lung thus leading to an increase in alveolar particle deposition (Corcoran and Gamard 2004, Gemci, et al. 2003, Kim and Corcoran 2009). These calculations are performed by replacing the density and dynamic viscosity of air with the property values for heliox. The density of 80/20 heliox is approximately 1/3 that of air and the dynamic viscosity is slightly higher than that of air. The heliox results are compared to the air results to determine if any enhancement in particle deposition occurs as a consequence of the differences in these properties. The effects of heliox on tidal volume and respiratory conditions that are suggested by Corcoran and Gamard (2004) are not taken into consideration.

5.2 Results and Discussion

Figure 18 shows the volume-weighted deposition for the heliox and air for human subjects. The difference in the results between air and heliox in this study appear to be insignificant. The use of heliox in place of air does not seem to have any effect on the volume-weighted deposition for the young children (3-years old and under). For the older ages presented in this study, the slight increase in particle deposition as a result of the heliox

is likely due to statistical error as a result of the all of the assumptions made in this study. In addition, no change in optimal particle size occurs as a result of the addition of heliox.

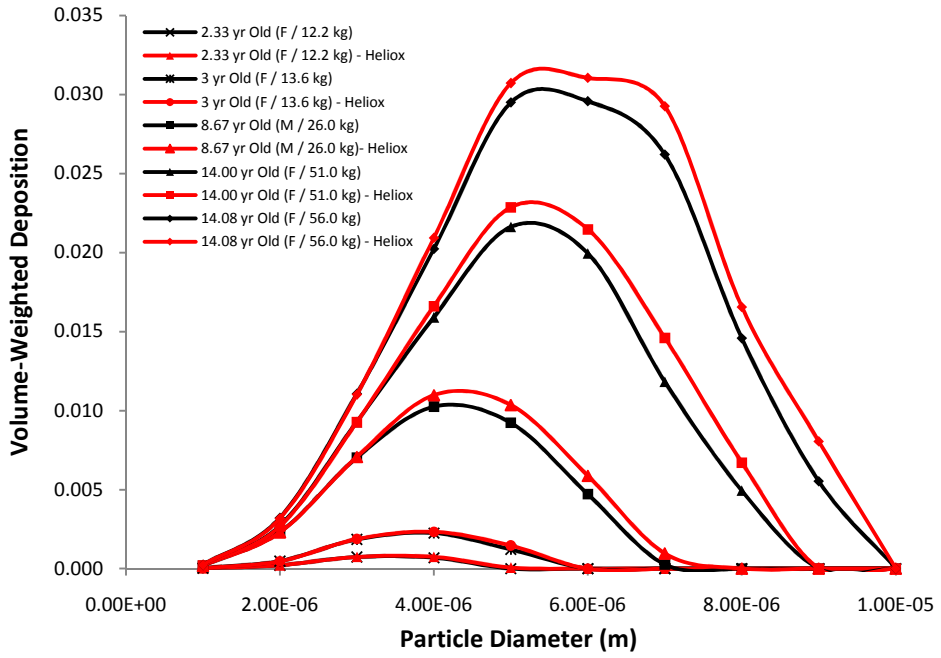

Figure 18: Volume-weighted AL deposition in humans with air and heliox

5.3 Conclusions

No apparent change in particle deposition efficiency in the alveolar region occurs in this study as a result of the differences between dynamic viscosity and density of air and heliox. Other property differences between air and heliox were not taken into consideration in this study, and there is a possibility that heliox might have beneficial effects as a result of factors not addressed in this study.

CHAPTER SIX: SUMMARY AND CONCLUSIONS

6.1 Model Summary

This study uses respiratory conditions, lung morphometry models, and lung volumes for humans and animal species, along with a static statistical mathematical model, to provide probabilities of alveolar deposition via inertial impaction, gravitational sedimentation, and Brownian motion. The human models used in this study include males and females ranging in age from 3-months old to 21-years old; the animal models in this study include the *B6C3F$_1$* mouse, the Long-Evans hooded rat, and the Beagle dog. As long as appropriate lung morphometry models, respiratory conditions, and lung volumes are available, this model can easily be used to determine deposition for other subjects.

6.2 Human Deposition, Optimal Particle Size, and Breathing Rate Conclusions

This study hypothesized that the optimal breathing rate and optimal particle size for volume-weighted deposition are dependent upon body weight, with both increasing as body weight increases. The results of this study verify that this hypothesis is correct. For volume-weighted alveolar deposition at normal breathing rates, the variation of optimal particle size is ~2.5 μm for infants to 5-6 μm for adults, which represents a two-fold increase in optimal particle size as age/body weight increase. Correlations are developed in this study that determine volume-weighted deposition and optimal particle size as a function of body weight. These correlations are shown below and can be used for both genders to determine

approximate volume-weighted deposition *VWD* and optimal particle diameter $d_{optimal}$ at normal breathing rates for subjects of a particular weight *W*.

$$d_{optimal}\ (\mu m) = 0.042 \cdot W\ (kg) + 2.774$$

$$VWD = 0.0005 \cdot W\ (kg) - 0.0034$$

The results of this study also indicate that slowing breathing rates below normal breathing rates, especially in children, enhances deposition performance. Also, the results indicate that optimal particle size shifts as a result of changes in breathing rate and this should be taken into consideration when developing delivery devices and delivering therapeutics.

The sensitivity analysis performed shows that for very young children, sensitivity of volume-weighted deposition to changes in breathing rate is greater than sensitivity to changes in particle diameter at normal breathing rates, and the sensitivity to both breathing rate and particle diameter are the lowest at the optimal breathing rate. For older children, the sensitivity of volume-weighted deposition to breathing rate is only slightly higher than sensitivity to particle diameter, exhibiting the lowest sensitivity to both at optimal breathing rates. For healthy adults, the magnitude of sensitivity of volume-weighted deposition to both breathing rate and particle diameter is similar regardless of breathing rate, and there does not appear to be a difference in sensitivity at the normal and optimal breathing rates.

6.3 Human and Animal Deposition and Optimal Particle Size Conclusions

This study hypothesized that the delivered dose (volume-weighted deposition) and optimal particle size will differ significantly between various animal species and humans.

When translating dose from an animal model to a human model, simply administering more drug for a higher body mass is determined in this study to be inappropriate and could potentially lead to over or under dosing. Despite considerable differences in body weight, each animal evaluated in this study surprising represents a human age group relatively well.

The results comparing deposition in humans and animals indicate that the mouse represents the traditional deposition efficiency, volume-weighted deposition, and optimal particle size for the 3-yr old female very well and is likely generally a good model of optimal particle size for younger children. The rat is likely a good model for older children based on the similarities in volume-weighted deposition to the 9.42-yr old. The canine, on the other hand, likely models adolescent humans reasonably well generally although it does not exactly match any of the subjects presented in this study. The rates of increase of deposition increase and optimal particle size as a function of mass, however, are different among the animals and the small human sample population represented in this study. The similarities and differences between humans and animal species need to be kept in mind in relation to therapeutic particle size and dosing.

Furthermore, it is obvious from the increase in volume-weighted deposition and the shift in optimal particle size that that deposition and optimal particle sizes for humans depend upon how the regions of the lung are defined. If the generations that are included in the alveolar region are changed, these results demonstrate that the deposition will change. Awareness of this is critical when determining and comparing deposition between various models. It is important to define similar lung regions for each model for the results to be accurately compared.

6.4 Heliox and Air Comparison Conclusions

This study hypothesized that heliox will lead to enhanced deposition when compared to air as a result of differences in density and dynamic viscosity. The results of this study determine that heliox has no apparent effect on particle deposition in the alveolar region when compared to air as a result of the differences in density and dynamic viscosity. However, other property differences between air and heliox were not taken into consideration in this study, and there is a possibility that heliox might have beneficial effects as a result of factors not addressed in this study.

6.5 Future Work

The results presented in this study only take into account one morphometric model for each represented age. Since lung geometry can vary significantly between individuals, additional research is needed to address the differences between individuals of each age group. Evaluation of results that apply a distribution to TV, TLC, FRC, MV, and airways dimensions would provide insight into variations that exist within the population. It is also valuable to evaluate the differences in optimal particle size and deposition between males and females of the same age and body weight. Additionally, more research is needed for adolescents and adults to determine if a relationship exists between BMI and optimal particle size or volume-weighted deposition since a limited number of subjects of these ages is presented in this study.

Numerous animal species not taken into consideration in this study are utilized in inhalation studies and dosing. However, lung morphometry and physiological information for many of these species is limited or not available. If this information were accessible, determination as to whether these animal species more accurately represent humans would be possible. Further studies are needed to determine morphometry and respiratory conditions for these various species to enable statistical particle deposition efficiency comparisons with humans.

Further, these results fail to capture that differences exist in inspiration and expiration rates. Moreover, clinical studies are needed to validate these statistical results because the models used in this study are static and fail to account for the dilation of the lung geometry during inspiration and expiration. It is only in models that can capture this aspect that the effects of lung remodeling as a result of disease can be explored.

REFERENCES

1. National Center for Health Statistics. *Clinical Growth Charts.* August 4, 2009. http://www.cdc.gov/growthcharts/clinical_charts.htm.

2. Asgharian, B., M. G. Ménache, and F. J. Miller. "Modeling Age-Related Particle Deposition in Humans." *J Aerosol Med* 17, no. 3 (2004): 213-224.

3. Bal, H. S., and N. G. Ghoshal. "Morphology of the terminal bronchiolar region of common laboratory mammals." *Lab Anim* 22 (1988): 76-82.

4. Bennett, W. D. "Variability of fine particle deposition in healthy adults: effects of age and gender." *Am J Resp Crit Care* 153, no. 5 (1996): 1641-1647.

5. Chan, T. L., and M. Lippmann. "Experimental Measurement and Empirical Modelling of the Regional Deposition of Inhaled Particles in Humans." *Am Ind Hyg Assoc J* 41 (1980): 399-409.

6. Cook, C. D., and J. F. Hamann. "Relation of Lung Volumes to Height in Healthy Persons Between the Ages of 5 and 38 Years." *J Pediatr* 59, no. 5 (1961): 710-714.

7. Corcoran, T. E., and S. Gamard. "Development of Aerosol Drug Delivery with Helium Oxygen Gas Mixtures." *J Aerosol Med* 17, no. 4 (2004): 299-309.

8. Dahl, A. R., R. B. Schlesinger, H. A. Heck, M. A. Medinsky, and G. W. Lucier. "Comparitive Dosimetry of Inhaled Materials: Differences among Animal Species and Extrapolation to Man." *Fund Appl Toxicol* 16 (1991): 1-13.

9. Davies, G., and L. Reid. "Growth of the alveoli and pulmonary arteries in childhood." *Thorax* 25 (1970): 669-681.

10. Dunhill, M. S. "Postnatal Growth of the Lung." *Thorax* 17 (1962): 329-333.

11. Finlay, W. H. *The Mechanics of Inhaled Pharmaceutical Aerosols: An Introduction.* San Diego, CA: Academic Press, 2001.

12. Finlay, W. H., C. F. Lange, M. King, and D. P. Speert. "Lung Delivery of Aerosolized Dextran." *Am J Resp Crit Care* 161 (2000): 91-97.

13. Gaultier, C., M. Boulé, Y. Allaire, A. Clément, and F. Girard. "Growth of Lung Volumes During the First Three Years of Life." *Bull Europ Physiopath Resp* 15, no. 6 (1979): 1103-1116.

14. Gemci, T., B. Shortall, G. M. Allen, T. E. Corcoran, and N. Chigier. "A CFD study of the throat during aerosol drug delivery using heliox and air." *J Aerosol Sci* 34, no. 9 (2003): 1175-1192.

15. Gradoń, L., and J. Marijnissen. *Optimization of Aerosol Drug Delivery.* Norwell, MA: Kluwer Academic Publishers, 2003.

16. Gupta, P. K., and A. J. Hickey. "Contemporary approaches in aerosolized drug delivery to the lung." *J Control Release* 17 (1991): 129-148.

17. Haefeli-Bleuer, B., and E. R. Weibel. "Morphometry of the Human Pulmonary Acinus." *Anat Rec* 220, no. 4 (4 1988): 401-414.

18. Hofmann, W. "Mathematical Model for the Postnatal Growth of the Human Lung." *Resp Physiol* 49 (1982): 115-129.

19. Hofmann, W. "Mathematical Model for the Postnatal Growth of the Human Lung." *Resp Physiol* 49 (1982): 115-129.

20. Hofmann, W., T. B. Martonen, and R. C. Graham. "Predicted Deposition of Nonhygroscopic Aerosols in the Human Lung as a Function of Subject Age." *J Aerosol Med* 2, no. 1 (1989): 49-68.

21. Horsfield, K., and G. Cumming. "Morphology of the Bronchial Tree in Man." *J Appl Phys* 24, no. 3 (03 1968): 373-383.

22. Hsieh, T. H., C. P. Yu, and G. Oberdörster. "Deposition and Clearance Models of Ni Compounds in the Mouse Lung and Comparisions with the Rat Models." *Aerosol Sci Tech* 31 (1999): 358-372.

23. Ingham, D. B. "Diffusion of Aerosols from a Stream Flowing Through a Cylindrical Tube." *J Aerosol Sci* 6 (1975): 125-132.

24. Kim, C. S. "Deposition of aerosol particles in human lungs: in vivo measurement and modelling." *Biomarkers* 14, no. S1 (2009): 54-58.

25. Kim, I. K., and T. Corcoran. "Recent Developments in Heliox Therapy for Asthma and Bronchiolitis." *Clinical Pediatric Emergency Medicine* 10, no. 2 (2009): 68-74.

26. Kleinstreuer, C., Z. Zhang, and J. F. Donohue. "Targeted Drug-Aerosol Delivery in the Human Respiratory System." *Annu Rev Biomed Eng* 10 (2008): 195-220.

27. Kliment, V. "Dichotomical Model of Respiratory Airways of the Rabbit and Its Significance for the Construction of Deposition Models." *Folio Morphologica* 22, no. 3 (1974): 286-290.

28. Kliment, V., J. Libich, and V. Kaudersova. "Geometry of Guinea Pig Respiratory Tract and Application of Landahl's Model of Deposition of Aerosol Particles." *J Hyg Epid Microb Im* 16 (1972): 107-114.

29. Kulkarni, V. S. *Handbook for Non-Invasive Drug Delivery Systems.* Burlington, MA: Elsevier, 2010.

30. Maina, J. N., and P. v. Gils. "Morphometric characterization of the airway and vascular systems of the lung of the domestic pig, Sus scrofa: comparison of the airway, arterial and venous systems." *Comp Biochem Phys A* 130 (2001): 781-798.

31. Malcolmson, R. J., and J. K. Embleton. "Dry Powder Formulations for Pulmonary Delivery." *Pharm Sci Technol To* 1, no. 9 (12 1998): 394-398.

32. Martonen, T. B., I. M. Katz, and C. J. Musante. "A Nonhuman Primate Aerosol Deposition Model for Toxicological and Pharmaceutical Studies." *Inhal Toxicol* 13 (2001): 307-324.

33. Martonen, T. B., Z. Zhang, and Y. Yang. "Interspecies Modeling of Inhaled Particle Deposition Patterns." *J Aerosol Sci* 23, no. 4 (1992): 389-406.

34. Mauderly, J. L. "Influence of Sex and Age on the Pulmonary Functino of the Unanesthetized Beagle Dog." *J Gerontol* 29, no. 3 (1974b): 282-289.

35. Ménache, M. G., W. Hofmann, B. Ashgarian, and F. J. Miller. "Airway Geometry Models of Children's Lungs for Use in Dosimetry Modeling." *Inhal Toxicol* 20 (2008): 101-126.

36. Newhouse, M. T., and R. E. Ruffin. "Deposition and Fate of Aerosolized Drugs." *CHEST* 73, no. 6 Suppl. (1979): 936-943.

37. Oldham, M. J., and R. J. Robinson. "Calculated Deposition in Growing Tracheobronchial Airways: Effect of Growth-Rate Assumptions." *Inhal Toxicol* 18 (2006): 803-808.

38. Oldham, M. J., and R. J. Robinson. "Predicted Tracheobronchial and Pulmonary Depositin in a Murine Asthma Model." *Anat Rec* 290, no. 10 (2007): 1309-1314.

39. Pedersen, S., J. C. Dubus, and G. Crompton. "The ADMIT series - Issues in Inhalation Therapy. 5) Inhaler selection in children with asthma." *Prim Care Respir J* 19, no. 3 (2010): 209-216.

40. Phalen, R. F. "An Airway Model for the Laboratory Mouse." Final research report submitted to NiPERA, November, 1991.

41. Phalen, R. F. *Inhalation Studies: Foundations and Techniques.* 2nd. New York: Informa Healthcare, 2009.

42. Phalen, R. F., and M. J. Oldham. "Methods for modeling particle deposition as a function of age." *Resp Physiol* 128 (2001): 119-130.

43. Phalen, R. F., and M. J. Oldham. "Tracheobronchial Airway Structure as Revealed by Casting Techniques." *Am Rev Respir Dis* 128, no. 2 (1983): S1-S4.

44. Phalen, R. F., H. C. Yeh, G. M. Schum, and O. G. Raabe. "Application of an Idealized Model to Morphometry of the Mammalian Tracheobronchial Tree." *Anat Rec* 190 (1978): 167-176.

45. Phalen, R. F., H. C. Yeh, O. G. Raabe, and D. J. Velasquez. "Casting the Lungs In-Situ." *Anat Rec* 177, no. 2 (1973): 255-264.

46. Phalen, R. F., M. J. Oldham, and R. K. Wolff. "The Relevance of Animal Models for Aerosol Studies." *J Aerosol Med Pulm D* 21, no. 1 (2008): 113-124.

47. Phalen, R. F., M. J. Oldham, C. B. Beaucage, T. T. Crocker, and JD Mortensen. "Postnatal Enlargement of Human Tracheobronchial Airways and Implications for Particle Deposition." *Anat Rec* 212, no. 4 (1985): 368-380.

48. Phillips, C. G., and S. R. Kaye. "Diameter-based analysis of the branching geometry of four mammalian bronchial trees." *Resp Physiol* 102 (1995): 303-316.

49. Praxair. *Physics of Heliox.* http://www.praxairexpress.org/praxair.nsf/7a1106cc7ce1c54e85256a9c005accd7/8afa98436a49654385256fcf004ccee2?OpenDocument.

50. Quanjer, P. H., G. J. Tammeling, J. E. Cotes, O. F. Pedersen, R. Peslin, and J. Yernault. "Lung Volumes and Forced Ventilatory Flows." *Eur Respir J* 6, no. Suppl. 16 (1993): 5-40.

51. Quanjer, P. H., J. Stocks, G. Polgar, M. Wise, J. Karlberg, and G. Borsboom. "Compilation of Reference Values for Lung Function Measurements in Children." *Eur Respir J* 2, no. Suppl. 4 (1989): 184s-261s.

52. Raabe, O. G., H. C. Yeh, G. M. Schum, and R. F. Phalen. *Tracheobronchial Geometry: Human, Dog, Rat, Hamster.* LF-53, Albuguerque, NM: Lovelace Foundation for Medical Education and Research, 1976.

53. Ruzer, L. S., and N. H. Harley. *Aerosols Handbook: Measurement, Dosimetry, and Health Effects.* Boca Raton, Fl: CRC Press, 2005.

54. Schlesinger, R. B. "Comparative Deposition of Inhaled Aerosols in Experimental Animals and Humans: A Review." *J Toxicol Env Health* 15, no. 2 (1985): 197-214.

55. Schlesinger, R. B., and L. A. McFadden. "Comparative Morphometry of the Upper Bronchial Tree in Six Mammalian Species." *Anat Rec* 199, no. 1 (1981): 99-108.

56. Schmid, O., et al. "Model for the Deposition of Aerosol Particles in the Respiratory Tract of the Rat." *J Aerosol Med Pulm D* 21, no. 3 (2008): 291-307.

57. Schum, M., and H. C. Yeh. "Theoretical Evaluation of Aerosol Deposition in Anatomical Models of Mammalian Lung Airways." *Bull Math Biol* 42 (1980): 1-15.

58. Stahlhofen, W., J. Gebhart, and J. Heyder. "Experimental determination of the regional deposition of aerosol particles in the human respiratory tract." *Am Ind Hyg Assoc J* 41, no. 6 (1980): 385-398.

59. Stocks, J., and P. H. Quanjer. "Reference Values for Residual Volume, Functional Residual Capacity and Total Lung Capacity." *Eur Respir J* 8 (1995): 492-506.

60. Taussig, L. M., T. R. Harris, and M. D. Lebowitz. "Lung Function in Infants and Young Children: Functional Residual Capacity, Tidal Volume, and Respiratory Rate." *Am Rev Respir Dis* 116, no. 2 (1977): 233-239.

61. Thurlbeck, W. M., and G. E. Angus. "Growth and Aging of the Normal Human Lung." *Chest* 67 (1975): 3S-7S.

62. Wang, B., T. Siahaan, and R. Soltero. *Drug Delivery: Principles and Applications.* Hoboken, NJ: John Wiley and Sons, Inc., 2005.

63. Weibel, E.R. *Morphometry of the Human Lung.* NY: Academic Press, 1963.

64. Weinberg, B. D., et al. "Mapping of PET-measured aerosol deposition: a comparison study." *J Aerosol Sci* 36 (2005): 1157-1176.

65. Xu, G. B., and C. P. Yu. "Effects of Age on Deposition of Inhaled Aerosols in the Human Lung." *Aerosol Sci Tech* 5, no. 3 (1986): 349-357.

66. Yeh, H. C. *Respiratory Tract Deposition Models.* LF-72, Albuquerque, NM: Lovelace Biomedical and Environmental Research Institute, 1980.

67. Yeh, H. C., and G. M. Schum. "Models of Human Lung Airways and Their Application to Inhaled Particle Deposition." *Bull Math Biol* 42 (1980): 461-480.

68. Yeh, H. C., G. M. Schum, and M. T. Duggan. "Anatomical Models of the Tracheobronchial and Pulmonary Regions of the Rat." *Anat Rec* 195, no. 3 (1979): 483-492.

69. Yu, C. P., L. Zhang, M. H. Becquemin, M. Roy, and A. Bouchikhi. "Algebraic Modeling of Total and Regional Deposition of Inhaled Particles in the Human Lung of Various Ages." *J Aerosol Sci* 23, no. 1 (1992): 73-79.

70. Zeltner, T. B., J. H. Caduff, P. Gehr, J. Pfenninger, and P. H. Burri. "The Postnatal Development and Growth of the Human Lung. I. Morphometry." *Resp Physiol* 67 (1987): 247-267.

APPENDIX A

Lung Morphometry for 0.25-year Old Human (Female)						
Generation #	Airway Type	Diameter (cm)	Length (cm)	Volume (cm^3)	Cumulative Volume (cm^3)	Number of Airways
0	CA	0.733	3.330	1.405	1.405	1
1	CA	0.550	1.580	0.751	2.156	2
2	CA	0.348	0.645	0.245	2.401	4
3	CA	0.231	0.470	0.158	2.559	8
4	CA	0.159	0.412	0.131	2.690	16
5	CA	0.116	0.388	0.131	2.821	32
6	CA	0.090	0.344	0.140	2.961	64
7	CA	0.068	0.291	0.135	3.096	128
8	CA	0.053	0.247	0.140	3.236	256
9	CA	0.043	0.177	0.132	3.367	512
10	CA	0.034	0.136	0.126	3.494	1,024
11	CA	0.028	0.102	0.129	3.623	2,048
12	CA	0.023	0.077	0.131	3.754	4,096
13	CA	0.020	0.059	0.152	3.905	8,192
14	CA	0.017	0.046	0.171	4.077	16,384
15	TB	0.015	0.038	0.220	4.297	32,768
16	RB	0.013	0.031	0.270	4.566	65,536
17	RB	0.012	0.027	0.400	4.966	131,072
18	RB	0.011	0.024	0.598	5.564	262,144
19	AD	0.010	0.021	0.865	6.429	524,288
20	AD	0.009	0.019	1.267	7.697	1,048,576
21	AD	0.008	0.018	1.897	9.594	2,097,152
22	AD	0.008	0.017	3.584	13.178	4,194,304
23	AS	0.007	0.016	5.165	18.343	8,388,608

(Ménache, et al. 2008)

Lung Morphometry for 1.75-year Old Human (Male)						
Generation #	Airway Type	Diameter (cm)	Length (cm)	Volume (cm^3)	Cumulative Volume (cm^3)	Number of Airways
0	CA	0.870	3.758	2.234	2.234	1
1	CA	0.643	1.780	1.156	3.390	2
2	CA	0.337	0.857	0.306	3.696	4
3	CA	0.217	0.589	0.174	3.870	8
4	CA	0.161	0.524	0.171	4.041	16
5	CA	0.135	0.573	0.262	4.303	32
6	CA	0.109	0.464	0.277	4.580	64
7	CA	0.089	0.374	0.298	4.878	128
8	CA	0.072	0.300	0.313	5.191	256
9	CA	0.057	0.232	0.303	5.494	512
10	CA	0.045	0.160	0.261	5.754	1,024
11	CA	0.037	0.115	0.253	6.008	2,048
12	CA	0.031	0.086	0.266	6.274	4,096
13	CA	0.026	0.066	0.287	6.561	8,192
14	CA	0.023	0.053	0.361	6.921	16,384
15	TB	0.020	0.044	0.453	7.374	32,768
16	RB	0.018	0.038	0.634	8.008	65,536
17	RB	0.016	0.034	0.896	8.904	131,072
18	RB	0.014	0.032	1.291	10.195	262,144
19	AD	0.013	0.030	2.088	12.283	524,288
20	AD	0.012	0.028	3.321	15.604	1,048,576
21	AD	0.012	0.027	6.404	22.008	2,097,152
22	AD	0.011	0.026	10.364	32.371	4,194,304
23	AS	0.010	0.026	17.130	49.501	8,388,608

(Ménache, et al. 2008)

Lung Morphometry for 1.92-year Old Human (Male)						
Generation #	Airway Type	Diameter (cm)	Length (cm)	Volume (cm^3)	Cumulative Volume (cm^3)	Number of Airways
0	CA	1.083	5.726	5.275	5.275	1
1	CA	0.745	2.175	1.896	7.171	2
2	CA	0.568	0.867	0.879	8.050	4
3	CA	0.361	0.622	0.509	8.559	8
4	CA	0.261	0.505	0.432	8.991	16
5	CA	0.202	0.507	0.520	9.511	32
6	CA	0.152	0.466	0.541	10.052	64
7	CA	0.122	0.386	0.578	10.630	128
8	CA	0.099	0.329	0.648	11.278	256
9	CA	0.080	0.269	0.692	11.971	512
10	CA	0.061	0.197	0.590	12.560	1,024
11	CA	0.050	0.147	0.591	13.151	2,048
12	CA	0.041	0.110	0.595	13.746	4,096
13	CA	0.034	0.084	0.625	14.371	8,192
14	CA	0.029	0.066	0.714	15.085	16,384
15	TB	0.024	0.053	0.786	15.871	32,768
16	RB	0.021	0.044	0.999	16.870	65,536
17	RB	0.018	0.037	1.234	18.104	131,072
18	RB	0.016	0.033	1.739	19.843	262,144
19	AD	0.014	0.029	2.341	22.184	524,288
20	AD	0.012	0.027	3.202	25.385	1,048,576
21	AD	0.011	0.025	4.982	30.368	2,097,152
22	AD	0.009	0.024	6.404	36.772	4,194,304
23	AS	0.008	0.023	9.698	46.470	8,388,608

(Ménache, et al. 2008)

Lung Morphometry for 2.33-year Old Human (Female)						
Generation #	Airway Type	Diameter (cm)	Length (cm)	Volume (cm^3)	Cumulative Volume (cm^3)	Number of Airways
0	CA	0.950	5.812	4.120	4.120	1
1	CA	0.858	2.390	2.764	6.883	2
2	CA	0.611	0.977	1.146	8.029	4
3	CA	0.498	0.541	0.843	8.872	8
4	CA	0.345	0.590	0.882	9.755	16
5	CA	0.271	0.543	1.002	10.757	32
6	CA	0.214	0.470	1.082	11.839	64
7	CA	0.169	0.396	1.137	12.976	128
8	CA	0.136	0.311	1.157	14.132	256
9	CA	0.119	0.288	1.640	15.772	512
10	CA	0.085	0.204	1.185	16.958	1,024
11	CA	0.068	0.160	1.190	18.148	2,048
12	CA	0.055	0.126	1.226	19.374	4,096
13	CA	0.045	0.099	1.290	20.664	8,192
14	CA	0.037	0.079	1.392	22.056	16,384
15	TB	0.030	0.064	1.482	23.538	32,768
16	RB	0.025	0.053	1.705	25.243	65,536
17	RB	0.021	0.044	1.998	27.240	131,072
18	RB	0.017	0.037	2.202	29.442	262,144
19	AD	0.014	0.032	2.583	32.025	524,288
20	AD	0.012	0.027	3.202	35.227	1,048,576
21	AD	0.010	0.024	3.953	39.180	2,097,152
22	AD	0.008	0.021	4.427	43.607	4,194,304
23	AS	0.007	0.019	6.134	49.741	8,388,608

(Ménache, et al. 2008)

Lung Morphometry for 3.00-year Old Human (Female)						
Generation #	Airway Type	Diameter (cm)	Length (cm)	Volume (cm^3)	Cumulative Volume (cm^3)	Number of Airways
0	CA	0.950	7.010	4.969	4.969	1
1	CA	0.701	2.275	1.756	6.725	2
2	CA	0.494	0.795	0.609	7.334	4
3	CA	0.397	0.596	0.590	7.925	8
4	CA	0.336	0.597	0.847	8.772	16
5	CA	0.267	0.531	0.951	9.723	32
6	CA	0.218	0.467	1.116	10.839	64
7	CA	0.176	0.395	1.230	12.069	128
8	CA	0.141	0.323	1.291	13.360	256
9	CA	0.111	0.236	1.169	14.529	512
10	CA	0.085	0.187	1.087	15.616	1,024
11	CA	0.068	0.144	1.071	16.687	2,048
12	CA	0.054	0.113	1.060	17.747	4,096
13	CA	0.044	0.090	1.121	18.868	8,192
14	CA	0.036	0.073	1.217	20.085	16,384
15	TB	0.030	0.060	1.390	21.475	32,768
16	RB	0.025	0.051	1.641	23.116	65,536
17	RB	0.021	0.044	1.998	25.113	131,072
18	RB	0.018	0.039	2.602	27.715	262,144
19	AD	0.016	0.035	3.690	31.404	524,288
20	AD	0.013	0.032	4.454	35.858	1,048,576
21	AD	0.012	0.029	6.878	42.736	2,097,152
22	AD	0.010	0.027	8.894	51.631	4,194,304
23	AS	0.009	0.026	13.875	65.506	8,388,608

(Ménache, et al. 2008)

Lung Morphometry for 8.67-year Old Human (Male)						
Generation #	Airway Type	Diameter (cm)	Length (cm)	Volume (cm^3)	Cumulative Volume (cm^3)	Number of Airways
0	CA	1.440	7.781	12.672	12.672	1
1	CA	1.045	3.375	5.789	18.461	2
2	CA	0.717	1.065	1.720	20.181	4
3	CA	0.513	0.798	1.320	21.501	8
4	CA	0.376	0.614	1.091	22.592	16
5	CA	0.288	0.695	1.449	24.041	32
6	CA	0.226	0.553	1.420	25.460	64
7	CA	0.178	0.428	1.363	26.824	128
8	CA	0.141	0.373	1.491	28.315	256
9	CA	0.111	0.262	1.298	29.613	512
10	CA	0.089	0.196	1.249	30.861	1,024
11	CA	0.074	0.148	1.304	32.165	2,048
12	CA	0.062	0.116	1.434	33.599	4,096
13	CA	0.052	0.095	1.653	35.252	8,192
14	CA	0.045	0.082	2.137	37.389	16,384
15	TB	0.040	0.073	3.006	40.395	32,768
16	RB	0.035	0.067	4.225	44.619	65,536
17	RB	0.031	0.063	6.233	50.852	131,072
18	RB	0.029	0.060	10.389	61.241	262,144
19	AD	0.026	0.058	16.145	77.386	524,288
20	AD	0.024	0.056	26.564	103.950	1,048,576
21	AD	0.022	0.055	43.846	147.796	2,097,152
22	AD	0.021	0.055	79.901	227.697	4,194,304
23	AD	0.020	0.054	142.309	370.006	8,388,608
24	AS	0.019	0.054	256.868	626.875	16,777,216

(Ménache, et al. 2008)

Lung Morphometry for 9.42-year Old Human (Male)						
Generation #	Airway Type	Diameter (cm)	Length (cm)	Volume (cm^3)	Cumulative Volume (cm^3)	Number of Airways
0	CA	1.647	9.921	21.136	21.136	1
1	CA	1.185	3.070	6.772	27.908	2
2	CA	0.727	1.130	1.876	29.784	4
3	CA	0.492	0.915	1.392	31.176	8
4	CA	0.387	0.746	1.404	32.580	16
5	CA	0.301	0.848	1.931	34.511	32
6	CA	0.234	0.675	1.858	36.369	64
7	CA	0.178	0.508	1.618	37.987	128
8	CA	0.132	0.408	1.429	39.416	256
9	CA	0.099	0.327	1.289	40.705	512
10	CA	0.081	0.221	1.166	41.871	1,024
11	CA	0.066	0.164	1.149	43.020	2,048
12	CA	0.055	0.127	1.236	44.256	4,096
13	CA	0.047	0.103	1.464	45.720	8,192
14	CA	0.041	0.088	1.904	47.624	16,384
15	TB	0.036	0.077	2.568	50.192	32,768
16	RB	0.033	0.071	3.980	54.172	65,536
17	RB	0.030	0.066	6.115	60.286	131,072
18	RB	0.028	0.063	10.169	70.456	262,144
19	AD	0.027	0.061	18.311	88.767	524,288
20	AD	0.025	0.059	30.368	119.135	1,048,576
21	AD	0.024	0.058	55.026	174.162	2,097,152
22	AD	0.024	0.057	108.155	282.317	4,194,304
23	AD	0.023	0.056	195.175	477.491	8,388,608
24	AS	0.022	0.056	357.144	834.635	16,777,216

(Ménache, et al. 2008)

Lung Morphometry for 14.00-year Old Human (Female)						
Generation #	Airway Type	Diameter (cm)	Length (cm)	Volume (cm^3)	Cumulative Volume (cm^3)	Number of Airways
0	CA	1.700	12.660	28.736	28.736	1
1	CA	1.196	3.050	6.853	35.589	2
2	CA	0.833	1.435	3.128	38.717	4
3	CA	0.623	1.116	2.722	41.438	8
4	CA	0.514	0.784	2.603	44.041	16
5	CA	0.398	0.817	3.253	47.294	32
6	CA	0.324	0.740	3.905	51.199	64
7	CA	0.259	0.572	3.857	55.056	128
8	CA	0.203	0.489	4.052	59.108	256
9	CA	0.159	0.390	3.965	63.072	512
10	CA	0.126	0.295	3.767	66.839	1,024
11	CA	0.102	0.227	3.799	70.638	2,048
12	CA	0.084	0.177	4.018	74.656	4,096
13	CA	0.071	0.143	4.638	79.294	8,192
14	CA	0.060	0.119	5.513	84.806	16,384
15	TB	0.052	0.102	7.098	91.904	32,768
16	RB	0.045	0.091	9.485	101.389	65,536
17	RB	0.040	0.082	13.506	114.896	131,072
18	RB	0.036	0.076	20.279	135.175	262,144
19	AD	0.033	0.072	32.286	167.461	524,288
20	AD	0.030	0.069	51.142	218.604	1,048,576
21	AD	0.028	0.066	85.228	303.831	2,097,152
22	AD	0.026	0.065	144.747	448.578	4,194,304
23	AD	0.024	0.063	239.080	687.658	8,388,608
24	AS	0.023	0.062	432.173	1119.830	16,777,216

(Ménache, et al. 2008)

Lung Morphometry for 14.08-year Old Human (Female)						
Generation #	Airway Type	Diameter (cm)	Length (cm)	Volume (cm^3)	Cumulative Volume (cm^3)	Number of Airways
0	CA	1.507	10.260	18.301	18.301	1
1	CA	1.478	3.630	12.456	30.756	2
2	CA	0.918	1.152	3.050	33.806	4
3	CA	0.724	0.777	2.559	36.365	8
4	CA	0.567	0.776	3.135	39.500	16
5	CA	0.460	1.052	5.595	45.095	32
6	CA	0.359	0.902	5.843	50.938	64
7	CA	0.281	0.677	5.374	56.312	128
8	CA	0.218	0.556	5.313	61.625	256
9	CA	0.165	0.424	4.642	66.267	512
10	CA	0.129	0.268	3.587	69.854	1,024
11	CA	0.102	0.185	3.096	72.950	2,048
12	CA	0.083	0.137	3.036	75.986	4,096
13	CA	0.069	0.110	3.370	79.355	8,192
14	CA	0.058	0.094	4.069	83.425	16,384
15	TB	0.050	0.086	5.533	88.958	32,768
16	RB	0.044	0.081	8.072	97.029	65,536
17	RB	0.039	0.077	12.056	109.086	131,072
18	RB	0.035	0.075	18.916	128.002	262,144
19	AD	0.032	0.074	31.203	159.204	524,288
20	AD	0.030	0.073	54.107	213.312	1,048,576
21	AD	0.028	0.073	94.267	307.578	2,097,152
22	AD	0.026	0.073	162.562	470.141	4,194,304
23	AD	0.025	0.072	296.478	766.618	8,388,608
24	AS	0.024	0.072	546.468	1313.086	16,777,216

(Ménache, et al. 2008)

Lung Morphometry for 18.00-year Old Human (Male)						
Generation #	Airway Type	Diameter (cm)	Length (cm)	Volume (cm^3)	Cumulative Volume (cm^3)	Number of Airways
0	CA	1.507	9.236	16.474	16.474	1
1	CA	1.478	3.535	12.130	28.604	2
2	CA	0.918	1.380	3.654	32.258	4
3	CA	0.724	0.865	2.849	35.106	8
4	CA	0.567	0.969	3.915	39.021	16
5	CA	0.460	0.969	5.153	44.174	32
6	CA	0.359	0.889	5.759	49.934	64
7	CA	0.281	0.770	6.112	56.046	128
8	CA	0.218	0.584	5.580	61.626	256
9	CA	0.165	0.496	5.430	67.056	512
10	CA	0.129	0.367	4.912	71.968	1,024
11	CA	0.102	0.278	4.652	76.620	2,048
12	CA	0.083	0.214	4.743	81.363	4,096
13	CA	0.069	0.169	5.177	86.540	8,192
14	CA	0.058	0.139	6.017	92.557	16,384
15	TB	0.050	0.117	7.528	100.084	32,768
16	RB	0.044	0.103	10.264	110.348	65,536
17	RB	0.039	0.093	14.562	124.910	131,072
18	RB	0.035	0.085	21.438	146.348	262,144
19	AD	0.032	0.080	33.733	180.081	524,288
20	AD	0.030	0.076	56.331	236.411	1,048,576
21	AD	0.028	0.073	94.267	330.678	2,097,152
22	AD	0.026	0.071	158.108	488.787	4,194,304
23	AD	0.025	0.069	284.125	772.911	8,388,608
24	AS	0.024	0.068	516.109	1289.020	16,777,216

(Ménache, et al. 2008)

Lung Morphometry for 21.00-year Old Human (Male)						
Generation #	Airway Type	Diameter (cm)	Length (cm)	Volume (cm^3)	Cumulative Volume (cm^3)	Number of Airways
0	CA	2.060	12.920	43.061	43.061	1
1	CA	1.670	3.620	15.858	58.920	2
2	CA	1.052	1.557	5.413	64.333	4
3	CA	0.778	1.134	4.313	68.646	8
4	CA	0.555	0.905	3.503	72.149	16
5	CA	0.398	0.919	3.659	75.808	32
6	CA	0.311	0.880	4.278	80.086	64
7	CA	0.234	0.848	4.668	84.754	128
8	CA	0.178	0.676	4.306	89.060	256
9	CA	0.131	0.533	3.678	92.738	512
10	CA	0.113	0.405	4.159	96.898	1,024
11	CA	0.093	0.292	4.062	100.960	2,048
12	CA	0.079	0.214	4.297	105.256	4,096
13	CA	0.068	0.164	4.879	110.135	8,192
14	CA	0.060	0.133	6.161	116.297	16,384
15	TB	0.054	0.114	8.555	124.852	32,768
16	RB	0.048	0.101	11.978	136.830	65,536
17	RB	0.044	0.094	18.734	155.564	131,072
18	RB	0.041	0.089	30.803	186.366	262,144
19	AD	0.038	0.085	50.541	236.908	524,288
20	AD	0.036	0.083	88.588	325.495	1,048,576
21	AD	0.034	0.081	154.228	479.723	2,097,152
22	AD	0.033	0.080	286.991	766.714	4,194,304
23	AD	0.032	0.080	539.722	1306.435	8,388,608
24	AS	0.031	0.079	1000.369	2306.804	16,777,216

(Ménache, et al. 2008)

Lung Morphometry for *B6C3F$_1$* Mouse						
Generation #	Airway Type	Diameter (cm)	Length (cm)	Volume (cm^3)	Cumulative Volume (cm^3)	Number of Airways
0	CA	0.137	0.897	0.0132	0.0132	1
1	CA	0.141	0.508	0.0159	0.0291	2
2	CA	0.114	0.202	0.0082	0.0373	4
3	CA	0.090	0.083	0.0042	0.0416	8
4	CA	0.078	0.097	0.0074	0.0490	16
5	CA	0.072	0.050	0.0065	0.0555	32
6	CA	0.063	0.043	0.0067	0.0622	50
7	CA	0.054	0.043	0.0074	0.0696	75
8	CA	0.045	0.040	0.0073	0.0769	115
9	CA	0.040	0.034	0.0075	0.0844	175
10	CA	0.036	0.033	0.0091	0.0934	270
11	CA	0.029	0.027	0.0075	0.1009	420
12	CA	0.021	0.024	0.0053	0.1062	640
13	CA	0.014	0.018	0.0027	0.1090	980
14	CA	0.010	0.013	0.0015	0.1105	1,505
15	TB	0.009	0.011	0.0021	0.1126	3,010
16	AD	0.009	0.010	0.0038	0.1164	6,020
17	AD	0.008	0.010	0.0061	0.1225	12,040
18	AD	0.008	0.010	0.0121	0.1346	24,080
19	AD	0.008	0.010	0.0242	0.1588	48,160
20	AD	0.008	0.010	0.0484	0.2072	96,320
21	AD	0.008	0.009	0.0871	0.2944	192,640

(Phalen 1991)

Lung Morphometry for Long-Evans Rat						
Generation #	Airway Type	Diameter (cm)	Length (cm)	Volume (cm^3)	Cumulative Volume (cm^3)	Number of Airways
0	CA	0.340	2.680	0.243	0.243	1
1	CA	0.290	0.715	0.094	0.338	2
2	CA	0.263	0.400	0.065	0.403	3
3	CA	0.203	0.176	0.028	0.431	5
4	CA	0.163	0.208	0.035	0.466	8
5	CA	0.134	0.117	0.023	0.489	14
6	CA	0.123	0.114	0.031	0.520	23
7	CA	0.112	0.130	0.049	0.569	38
8	CA	0.095	0.099	0.046	0.615	65
9	CA	0.087	0.091	0.059	0.674	109
10	CA	0.078	0.096	0.084	0.758	184
11	CA	0.070	0.073	0.087	0.845	309
12	CA	0.058	0.075	0.103	0.948	521
13	CA	0.049	0.060	0.099	1.047	877
14	CA	0.036	0.055	0.083	1.130	1,477
15	TB	0.020	0.035	0.027	1.157	2,487
16	AD	0.017	0.029	0.033	1.190	4,974
17	AD	0.016	0.025	0.050	1.240	9,948
18	AD	0.015	0.022	0.077	1.317	19,896
19	AD	0.014	0.020	0.123	1.440	39,792
20	AD	0.014	0.019	0.233	1.673	79,584
21	AD	0.014	0.018	0.441	2.114	159,168
22	AD	0.014	0.017	0.833	2.947	318,336
23	AS	0.014	0.017	1.666	4.613	636,672

(Yeh, Schum and Duggan 1979)

Lung Morphometry for a Beagle Dog						
Generation #	Airway Type	Diameter (cm)	Length (cm)	Volume (cm^3)	Cumulative Volume (cm^3)	Number of Airways
0	CA	1.800	14.800	37.66	37.661	1
1	CA	1.490	1.380	4.81	42.474	2
2	CA	1.160	1.520	4.82	47.293	3
3	CA	0.879	0.989	3.00	50.294	5
4	CA	0.605	0.847	1.95	52.242	8
5	CA	0.472	0.547	1.24	53.486	13
6	CA	0.399	0.443	1.16	54.649	21
7	CA	0.377	0.370	1.45	56.095	35
8	CA	0.345	0.400	2.13	58.226	57
9	CA	0.329	0.320	2.58	60.811	95
10	CA	0.300	0.287	3.21	64.016	158
11	CA	0.264	0.256	3.67	67.687	262
12	CA	0.220	0.289	4.77	72.455	434
13	CA	0.191	0.191	3.95	76.401	721
14	CA	0.176	0.162	4.71	81.111	1,195
15	CA	0.141	0.159	4.92	86.034	1,983
16	CA	0.114	0.154	5.17	91.205	3,290
17	CA	0.092	0.124	4.50	95.704	5,458
18	CA	0.074	0.103	4.01	99.715	9,054
19	CA	0.052	0.094	3.00	102.713	15,019
20	CA	0.044	0.081	3.70	106.413	30,038
21	TB	0.036	0.071	4.34	110.755	60,076
22	AD	0.031	0.063	5.71	116.468	120,152
23	AD	0.027	0.055	7.57	124.035	240,304
24	AD	0.025	0.049	11.56	135.595	480,608
25	AD	0.023	0.043	17.17	152.768	961,216
26	AD	0.022	0.038	27.77	180.537	1,922,432
27	AD	0.022	0.033	48.23	228.769	3,844,864
28	AD	0.021	0.029	77.24	306.008	7,689,728
29	AS	0.021	0.026	138.50	444.506	15,379,456

(Yeh 1980)